JOC The Journal of Organic Chemistry

Article

Long-Range Reactivity Modulations in Geranyl Chloride Derivatives

Michael B. Reardon, Muyun Xu, Qingzhe Tan, Peter G. Baumgartel, Danielle J. Augur, Shuanghong Huo, and Charles E. Jakobsche

J. Org. Chem., **Just Accepted Manuscript** • DOI: 10.1021/acs.joc.6b01759 • Publication Date (Web): 05 Oct 2016

ACS Publications

The Journal of Organic Chemistry is published by the American Chemical Society. 1155 Sixteenth Street N.W., Washington, DC 20036

Long-Range Reactivity Modulations in Geranyl Chloride Derivatives

Michael B. Reardon, Muyun Xu, Qingzhe Tan, Peter G. Baumgartel, Danielle J. Augur, Shuanghong Huo, Charles E. Jakobsche*

*corresponding author

Address and Contact Information
Carlson School of Chemistry & Biochemistry
Clark University
950 Main Street
Worcester, MA 01610 USA
email: cjakobsche@clarku.edu
phone: 508-793-8866
fax: 508-793-7117

TOC graphic

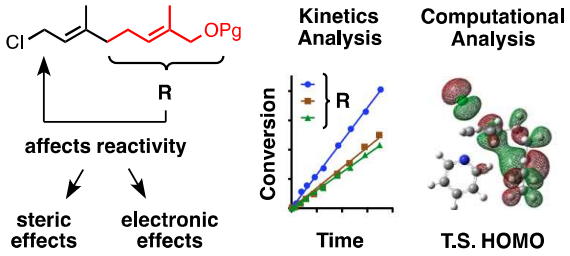

Abstract

Derivatives of geraniol are versatile synthetic intermediates that are useful for synthesizing a variety of terpenoid natural products; however, the results presented herein show that subtle differences in the structures of functionalized geranyl chlorides can significantly impact their abilities to function as effective electrophiles in synthetic reactions. A series of focused kinetics experiments identify specific structure–activity relationships that illustrate the importance not only of steric bulk, but also of electronic effects from distant regions of the molecules that contribute to their overall levels of reactivity. Computational modeling suggests that destabilization of the reactant by filled–filled orbital mixing events in some, but not all, conformations may be a critical contributor to these important electronic effects.

Introduction

The large and remarkably diverse family of naturally occurring terpenoid molecules,[1] many of which possess a variety of biological activities, have served as targets and motivation to synthetic chemists for several decades.[2,3,4] Since terpene biosynthesis utilizes oligoprenyl pyrophosphates as synthetic precursors,[1] a variety of cyclic terpene subfamilies retain these prenyl units in their final structures (Figure 1). The casbenes,[5] the dolabellanes,[6] and the germacrenes,[7] for example, each contain a geranyl unit (the 10-carbon fragments highlighted in red in Figure 1) that is connected to the rest of the structure by each of its two terminal carbon

atoms. The prevalence of this motif in a variety of potential target structures suggests that synthon **1**, a geranyl unit with an extra functional group on its terminal carbon, should be a broadly useful synthetic precursor. Indeed, these compounds have recently been utilized as synthetic intermediates in total syntheses of sarcophytonolide H,[8] oridamycin B,[9] and partheonolide,[10] as well as a terpenoid-like *trans*-bicyclic structure made by us.[11]

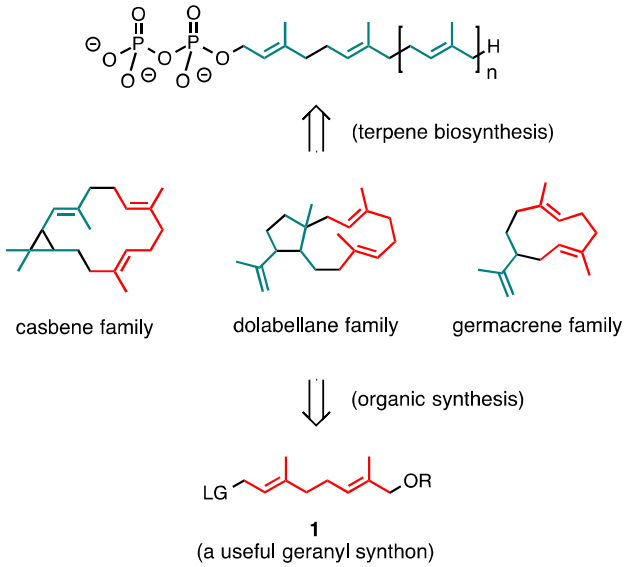

Figure 1. Representative terpene families, their biosynthetic precursors, and an important intermediate for their organic syntheses. Geranyl units are indicated in red, and prenyl units are indicated in teal. LG = leaving group.

In this paper we analyze how synthon **1**'s electrophilic reactivity varies depending on subtle changes to its structure, specifically on how that reactivity is affected by the presence of the second alkene and the nature of the extra functional group on its far end. The results show that the extra group does substantially impact the compound's overall reactivity even though it is quite far from the electrophilic site. Previously, with the goal of synthesizing particular diterpeneoid compounds from the dolabellane family, we developed a regio- and stereo-selective alkylation reaction between ketone **2** and geranyl chloride (Figure 2, R = H).[12] Although this reaction produces a single isomer of product **6** in a reasonable yield of 56%, our current line of inquiry has led us to discover that analogous reactions with functionalized derivatives of geraniol provide substantially lower yields. Specifically, OTBS- and OTHP-functionalized geranyl chlorides **4–5** produce only 2/3 or less than 1/2 as much product, respectively, compared to the reaction of the parent geranyl chloride (Figure 2). Since ketone **2** (but not products **6–8**) gradually decomposes under these strongly basic conditions, the rate of alkylation is critically connected to the yield of product in this reaction. Although there are numerous well-known examples of electrophiles whose reactivities are modulated by groups on distant regions of those molecule,[13,14,15] we found the differences in reaction efficiency in our system to be both surprising and interesting because although the R groups are bulky and electron-withdrawing, they are located quite far – eight bonds away – from the reactive site on a non-conjugated and highly flexible molecule.

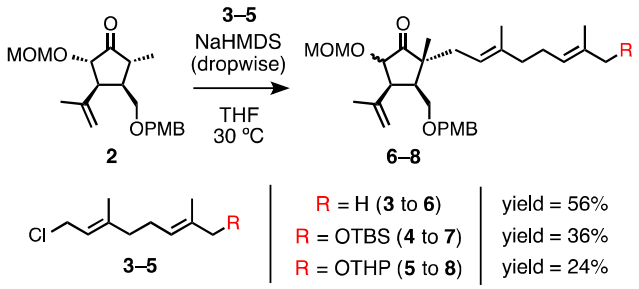

Figure 2. Effect of distal substituents on the alkylation of ketone **2**.

Results and Discussion

Initial Kinetics Analysis

We hypothesized that a more precise comparison of the reaction rates of these electrophiles would enable a more detailed understanding of how these distal functional groups are able to so dramatically affect the reactivities of these geranyl chloride derivatives. To directly compare the electrophilic reaction rates of geranyl chlorides **3**–**5**, we reacted each with pyridine and used ^{1}H NMR to monitor these reactions over time (Figure 3A, B). Compared to the alkylations of ketone **2**, the alkylations with pyridine are simpler and can be monitored more directly because they do not require additional reagents, complicating acid–base steps, or rigorously dry reaction conditions. The geranyl pyridinium products (**9**–**11**) are easily identifiable by their NMR signals, which can be monitored over time to assess the percent conversion of the geranyl chlorides (Supplementary Sections 1.4–1.5). Our experimental setup uses an excess of pyridine, which causes the pyridine's concentration to remain approximately constant and causes the reaction to exhibit pseudo-first-order kinetics. As expected, plots of [-ln(% unreacted geranyl chloride)] show linear increases over time during the initial 15 hours of the reaction (Supplemental Figure S8), during which time >90% of the geranyl chloride is consumed. According to first-order kinetics theory, the reaction rate constant (k) can be calculated by dividing the slopes of these plots by the initial (pseudo constant) concentration of the pyridine nucleophile, which we kept equivalent in each of our experiments. Therefore, the relative rates of two electrophiles can be easily calculated by directly comparing the slopes of two reactions (which we always performed in side-by-side conditions). Most of our experiments use 6–9 hour durations, after which time the differences in rates are readily observable (Figure 3C and Supplementary Figures S1–S6).

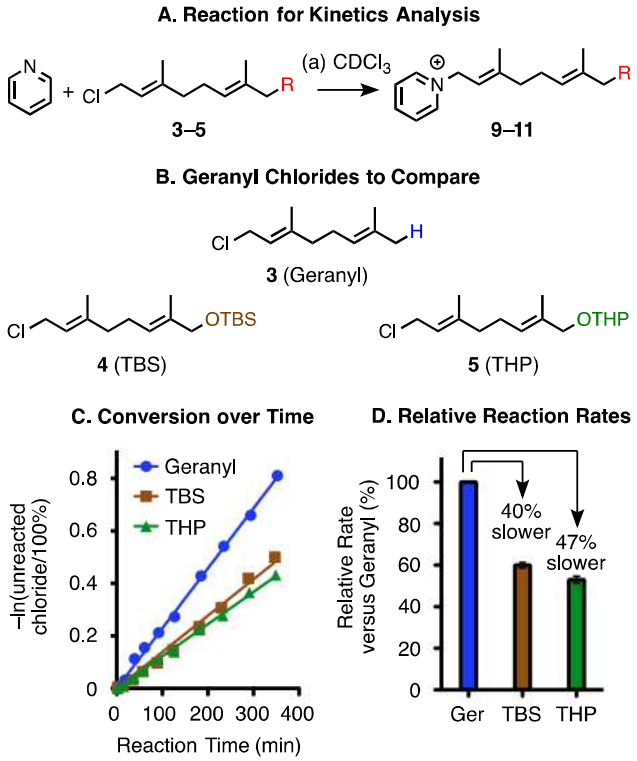

Figure 3. Kinetics analysis of geranyl chloride and two derivatives. A. Overview of the reaction to be studied. Conditions: (a) allylic chloride (1 equiv = 0.21 M in $CDCl_3$), pyridine (3 equiv = 0.63 M), 24 +/- 0.5 ºC, monitored by ^1H NMR. B. Structures of the three allylic chlorides to be compared. C. Comparison of the amount of conversion of chloride starting material into pyridinium product over time from a representative experiment. D. Comparison of the relative rates of reaction. Averages of two separate side-by-side comparisons. Error bars represent standard deviations from duplicate experiments.

Comparing the relative rate constants from geranyl chlorides **3**–**5** (averages of two separate side-by-side comparisons, Figure 3D) shows that the presence of the OTBS group reduces the reactivity by 40%, and the presence of the OTHP group reduces the reactivity by 47% in this reaction. These trends are qualitatively consistent with the lower yields observed for these electrophiles in the ketone-alkylation reaction described above. Clearly, these groups do substantially impact the electrophilic reactivities of these molecules despite being eight bonds away from the reactive carbon atom and not being connected to it by conjugation.

Focused Kinetics Experiments

From these initial rate comparison results, it is unclear whether steric or electronic contributions from the OTBS and OTHP groups are the major causes for the observed differences in reactivity. Although each of these groups is relatively bulky, the flexibility and length of the geranyl core should allow a variety of conformations, some of which position the bulk in non-influential locations. Also, although each of these groups is inductively electron-withdrawing, it is unlikely that polarization of sigma bonds would substantially impact the

electron density at the reaction center from such a distance. To distinguish the impact of steric and electronic components, we designed and synthesized additional geranyl chloride analogues that would enable less-ambiguous comparisons to be made.

First, to study the isolated effects of steric bulk, we synthesized lengthened geranyl chloride **16** and monounsaturated geranyl chloride analogue **22** (Scheme 1). The key step for synthesizing lengthened analogue **16**, which has an extra ethyl group added to the far end, is the alkylation of bromide **13** with sulfone **14** to incorporate the two extra carbon atoms. Bromide **13** can be accessed from alcohol **12**, which can be formed by a known allylic oxidation of geranyl acetate.[16] The key step for forming monounsaturated analogue **22**, which lacks the double bond at its far end, is a Horner–Wadsworth–Emmons olefination of ketone **19** (Scheme 1B). This reaction favors the desired *E* isomer, and this product can be separated from the minor *Z* isomer by column chromatography. Ketone **19** is accessed from a nickel-mediated coupling[17] between methyl vinyl ketone (**17**) and isobutyl iodide (**18**). Although the yield of this step is low, since it is the first step and can be done on a multi-gram scale with readily available materials, sufficient material can be obtained to complete the synthesis.

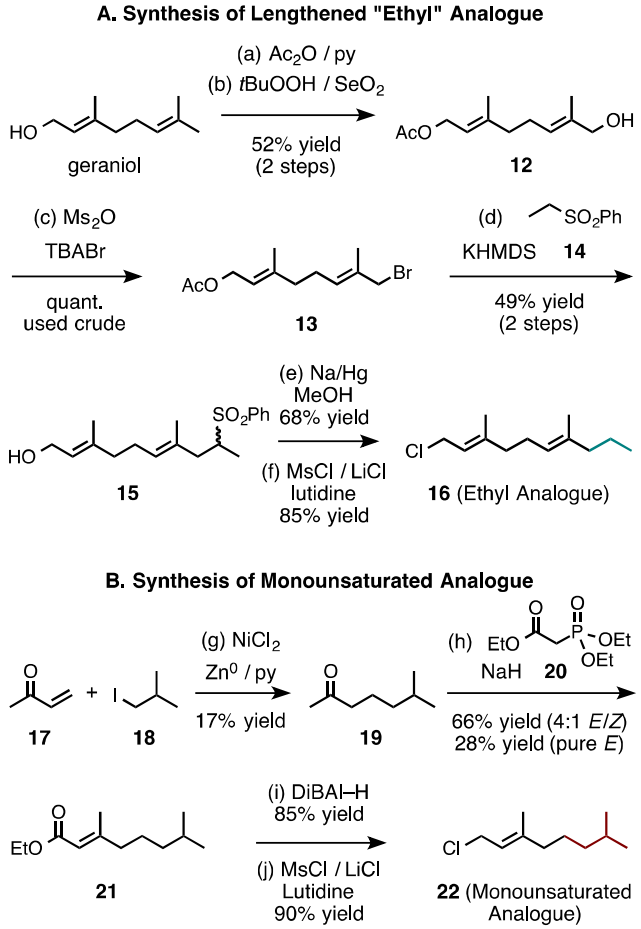

Scheme 1. Synthesis of geranyl chloride analogues **16** and **22**. Conditions: (a, b) See reference 16, 52% (2 steps); (c) DCM (0.4 M), 0 °C, 2,6-lutidine (3 equiv), tetrabutylammonium bromide (2.5 equiv), Ms_2O (1.5 equiv), 4 h, quant.; (d) sulfone **14** (4 equiv), THF (0.08 M), 0 °C, KHMDS (3 equiv), 30 min, then **13**, 3 h, 49% (2 steps); (e) MeOH (0.1 M), 0 ºC, 20% Na/Hg

(20 equiv), to ambient temp., 4 h, 68%; (f) LiCl (1.2 equiv, dried), DMF (0.25 M), 2,6-lutidine (4 equiv), methanesulfonyl chloride (2 equiv), 85%; (g) $NiCl_2$•$6H_2O$ (0.4 equiv), heat under vacuum, zinc (2.2 equiv), 2:1 THF/pyridine, methyl vinyl ketone (2 equiv), reflux (1.5 h), to ambient temp., 1-iodo-2-methylpropane (1 equiv), 30 min, reflux (16 h), 17%; (h) NaH (2 equiv), THF, 0 ºC, ester **20** (2.2 equiv), 30 min, then ketone **19**, THF (final conc. 0.09 M), to ambient temp., 17 h, 66% overall yield (4:1 *E*/*Z*), 28% yield of pure *E* after chromatography; (i) DCM (0.3 M), -84 ºC, DiBAl–H (3 equiv), 1 h, 85%; (j) LiCl (1.2 equiv, dried), DMF (0.25 M), 2,6-lutidine (2.5 equiv), methanesulfonyl chloride (2 equiv), 90%.

These monounsaturated and ethyl analogues enable direct structure–activity comparisons with prenyl chloride and geranyl chloride, respectively, to measure the effects of increasing steric bulk at the far end of the molecules without simultaneously withdrawing electron density (Figure 4A). Pyridine-alkylation experiments analogous to those described above were used to compare the relative reactivities of these electrophiles under pseudo-first-order conditions (Supplementary Figures S3–S6). Monounsaturated analogue **22** reacts 27% more slowly than prenyl chloride (**23**, Figure 4B), which suggests that the hydrocarbon chain is able to fold into 3-dimensional shapes that position the extra steric bulk close enough to the chloride-bearing carbon atom to have a meaningful impact on its reactivity as an electrophile. Furthermore, elongated ethyl analogue **16** reacts 16% more slowly than geranyl chloride, which further shows that the far regions of these molecules – which would be approximately one nanometer from the reactive site in an unfolded, linear conformation – are in fact still able to impact reactivity, presumably due to the importance of folded states that occur even in non-polar solvents such as chloroform.

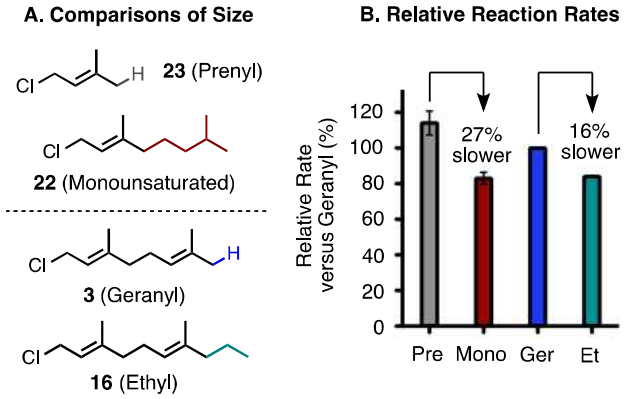

Figure 4. Impact of steric bulk on reaction rate. A. Structures to compare. B. Comparison of the relative rates of reaction. Averages of two separate side-by-side comparisons at either 23 +/- 0.5 or 24 +/- 0.5 ºC. Error bars represent standard deviations from duplicate experiments.

Next, to study the importance of electronic effects, we compared the reaction rates of pairs of isosteric molecules, which have similar sizes and shapes as each other yet possess different electronic properties on their distal ends (Figure 5A). The relative rates of their pseudo-first-order S_N2 reactions with excess pyridine (Figure 5B, Supplementary Figures S3–S6) show that monounsaturated analogue **22** reacts 17% more slowly than geranyl chloride itself. Since these molecules have similar shapes and sizes, the difference in rate suggests that the presence of the alkene on the far end of these molecules is able to enhance their rates of reaction despite not

being directly conjugated to the allylic chloride. Comparing the rates of elongated ethyl analogue **16** and methoxy-functionalized geranyl chloride **24** (see Supplementary Scheme S1 for synthesis), which are analogous in size and shape, shows that the methoxy geranyl chloride, whose second alkene is less electron rich due to the inductively electron-withdrawing nature of the methoxy group, reacts 16% more slowly.

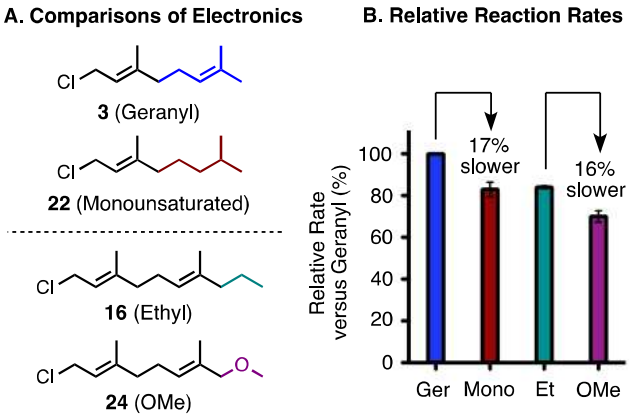

Figure 5. Impact of electronics on reaction rate. A. Structures to compare. B. Comparison of the relative rates of reaction. Averages of two separate side-by-side comparisons at either 23 +/- 0.5 or 24 +/- 0.5 ºC. Error bars represent standard deviations from duplicate experiments.

Taken together, these comparisons suggest that the presence of an electron-rich alkene on the non-reactive side of geranyl chloride helps to enhance its reactivity as an electrophile. We initially hypothesized that this rate enhancement could result from the distal π bond being able to donate electron density towards the electrophilic portion of the molecule, and thus being able to help stabilize a partial positive charge in the S_N2 transition state. We further hypothesized that this donation of electron density could occur by a through-space orbital-mixing interaction[18] that could exist in one or more of the folded conformations that are relevant to these geranyl structures. Alternatively, we thought it could also be possible that the π and π* orbitals of the two alkene groups could participate in hyperconjugation interactions[19] with the sigma bonds that connect them, thus allowing the two alkenes to interact with each other "through" the connecting single bonds.

Computational analysis

To help clarify the electronic effects created by geranyl chloride's distal alkene, we used computational modeling to evaluate and compare the reactant and transition-state structures of prenyl and geranyl chloride. Prenyl chloride is a relatively small compound with minimal conformational flexibility, and for its reactant and transition state we were able to find one energy-minimized geometry for each. Using Gaussian 09,[20] ground state geometries were found using the B3LYP functional[21] and the 6-311g(d) basis set[22] with the PCM solvation model[23] for dichloromethane. Transition-state geometries were found using the Berny method at the same level of theory, and energies for both these structures were calculated using the M06-2X method[24] with the 6-31+g(d,p) basis set[25] and the same solvation method. These same basis sets

have been previously used by Clement and Houk to analyze the structures and energies of transition states for proline-catalyzed aldol reactions.[26] Unlike prenyl chloride, which has minimal conformational flexibility, geranyl chloride can adopt several conformations. Using the Molecular Operating Environment 2015.10 program[27] with the LowModeMD method[28] and the Amber10:EHT forcefield,[29] we identified 14 unique energy minima (excluding enantiomeric conformations). For further analysis, we selected four of these conformations that seem to encompass most of the macroscopic diversity of the 14 total conformations (Figure 6). Using analogous computational methods, we were also able to find an energy-minimized geometry for each of these four reactants and transition states.

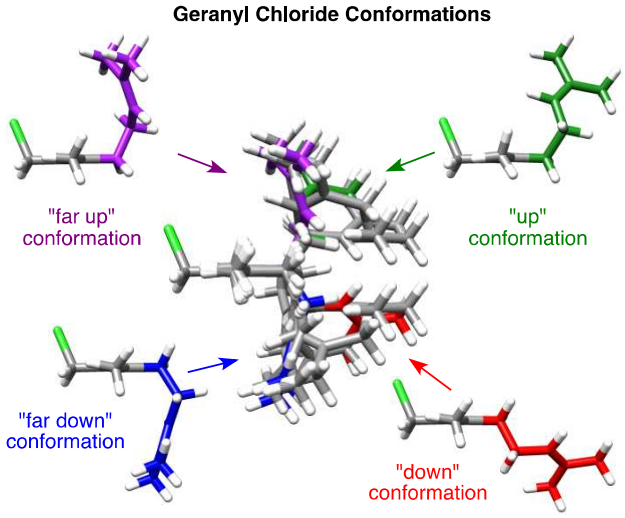

Figure 6. Conformations of geranyl chloride. Fourteen conformations, which each correspond to a free-energy minimum, are overlaid. The four conformations selected for further analysis are highlighted in colors and given nicknames. Structure overlapping and visualization was performed using the UCSF Chimera Package 1.10.2.[30]

We focused our analysis on the HOMO and HOMO-1 orbitals, among which there is notable variation between prenyl chloride and the four conformations of geranyl chloride. In contrast, visual inspection of the LUMO and lower-energy filled orbitals (HOMO-2 through HOMO-8) shows minimal variation between those orbitals from the five reactants or transition states (Supplementary Figures S9, S12, and S15–S17). For two of the four geranyl chloride reactant conformations (labeled "far down" and "far up"), the HOMO-1 orbitals resemble prenyl chloride's HOMO orbital in that the majority of the orbital's volume is located around the alkene adjacent to the chloride atom (Figure 7A). In the other two conformations (labeled "up" and "down"), however, the HOMO-1 orbitals encompass both alkene groups with approximately equal volumes. A similar trend can be seen in the HOMO of the four geranyl chloride reactant conformations; in the far-down and far-up conformations the volumes of the orbitals are localized around the distal alkene group, whereas in the down and up conformations the volumes encompass both alkenes (Figure 7B left side). In the HOMO and HOMO-1 of the geranyl chloride transition states, each of the four conformations has orbitals that extend over both alkene groups, yet the relative volumes around each alkene vary among the four conformations (Figure 7B right side, and Supplementary Figures S13–S14).

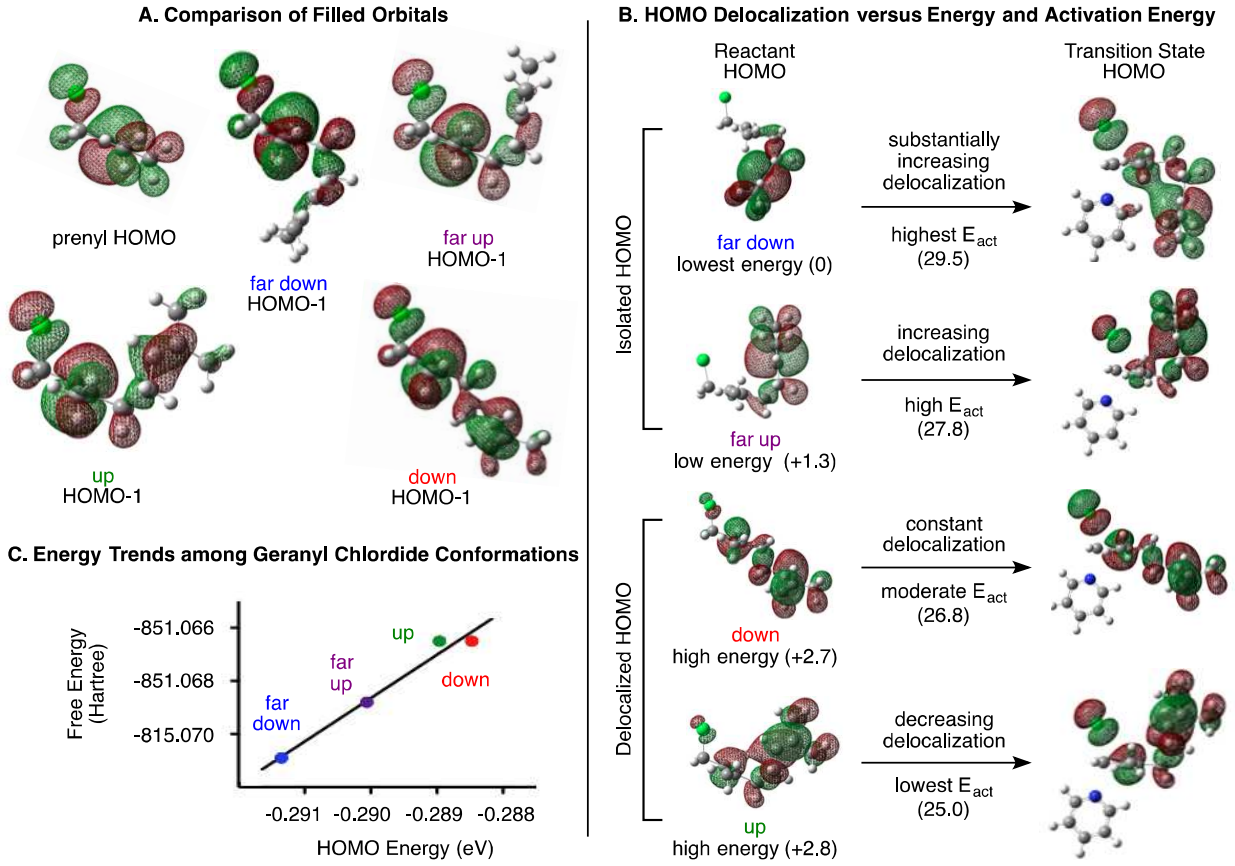

Figure 7. Calculated orbitals and energies. A. Filled orbitals from prenyl chloride or geranyl chloride reactants. B. Changes in HOMOs as different conformations of geranyl chloride react. Free energies of activation (E_{act}) are listed in kcal/mol. Free energies of the starting materials are listed in kcal/mol relative to the far-down conformation. C. Comparison of HOMO energy levels and free energies in geranyl chloride reactant conformations.

While the HOMO and HOMO-1 orbitals that are localized around individual alkene groups can be thought of as essentially being isolated π bonding orbitals, the other ones, which encompass both alkenes, can instead be thought of as linear combinations of the two π bonding orbitals mixing together and "delocalizing" across both alkene groups. Since this mixing interaction occurs between two filled orbitals, it should increase the energy of the HOMO and destabilize the molecule in conformations that enable more mixing. Another example of destabilizing orbital-mixing interactions between two filled orbitals is the n)(π repulsive interaction that has been identified to destabilize some conformations of proline mimics.[31] Among the four geranyl chloride conformations, a couple distinct correlations, which are described below, support this interpretation.

Among the four conformations of the geranyl chloride reactant, the amount of delocalization in the HOMOs correlates with the relative energies of those orbitals as well as with the relative free energies of the conformations such that more mixing corresponds to higher-energy orbitals

and structures (Figure 7B left side and Supplemental Table S2). The direct relationship between the relative energies of the HOMOs and the relative free energies of the structures, such that conformations with higher energy HOMOs also have higher free energies (Figure 7C), supports the idea that these orbital-mixing interactions are important contributors to the overall properties and reactivities of these molecules. The two conformations with minimal delocalization (far up and far down) have lower energies, and the two conformations with substantial delocalization (up and down) have higher energies (+2.7 and +2.8 kcal/mol versus the free energy of the far-down conformation). Interestingly, the two highly folded conformations (whose two π bonds are near each other in space) have less delocalization than the two less-folded conformations, which suggests that these orbital-mixing effects are not "through-space" interactions.

Additional correlations between orbital delocalization and free energies can also be seen from the transition-state structures. Free energies of activation for each geranyl chloride conformation were calculated as the difference between the free energy of the transition state and the sum of the free energies of the reactants (geranyl chloride and pyridine, calculated individually). The four conformations differ substantially in their activation energies (25.0–29.5 kcal/mol), and again these energies correlate to the delocalization of the HOMO; specifically, they correlate to how the amount of delocalization changes between the starting material and the transition state (Figure 7B). The amount of HOMO delocalization in the far-down conformation increases substantially from almost none in the starting material to a large amount (the most of all the conformations) in the transition state. Of the four, this conformation has the lowest energy starting material (with no destabilizing orbital mixing), but the highest energy transition state (with much destabilizing orbital mixing), which causes this conformation to have the highest activation energy (29.5 kcal/mol). The amount of HOMO delocalization in the far-up conformation increases from the starting material to the transition state, but not as much as it does in the far-down conformations, and this conformation has the second highest activation energy (27.8 kcal/mol). The amount of HOMO delocalization in the down conformation remains approximately constant, and it has the second smallest activation energy (26.8 kcal/mol). And finally, the amount of HOMO delocalization in the up conformation actually decreases from the starting material to the transition state (in which the 0.02 isovalue volumes around the two π bonds can be seen to no longer connect in the transition state), and this conformation has the smallest activation energy (25.0). Indeed, the activation energy for this conformation is similar to that calculated for the fast-reacting prenyl chloride (24.0 kcal/mol).

Conclusion

In conclusion, we present herein a combination of kinetics and computational analyses to help understand the difference in reactivity among various geranyl chloride derivatives that are relevant to total syntheses of numerous terpenoid natural products. Comparative analyses of relative reaction rates show that both steric and electronic factors influence the reactivities of these terminally functionalized geranyl chlorides. The impact of increased steric bulk on distal regions of the electrophile shows the importance of folded conformations to these molecules. While from the electronic perspective, the presence of an electron-rich alkene on the distal region of the molecule increases its electrophilic reactivity versus compounds that lack the second alkene or only have an electron-poor one. Computational analysis suggests that the enhanced electrophilic reactivity results from the fact that some, but not all, of geranyl chloride's

conformations enable repulsive π–π orbital-mixing interactions that can selectively destabilize the reactants more than the corresponding transition states. Thus, for the synthetic chemist, being aware of how bulky and electron-withdrawing groups can affect these types of electrophiles, even when they are far from the electrophile's reactive site, can help enable the development and optimization of synthetic reactions that involve geranyl electrophiles or related reagents.

Experimental Section

*General Procedure for Alkylating Ketone **2** with Allylic Chlorides.* Into a flame-dried flask were added ketone **2** (1 equiv), the required geranyl chloride (2.5 equiv), and toluene. Volatiles were removed under reduced pressure to remove any traces of water. The flask was fit with a condensing column, capped with a rubber septum, and maintained under a nitrogen atmosphere. THF was added, and the mixture was warmed to 30 ºC in an oil bath. Sodium hexamethyldisilazide (1.0 M in THF, 1.5 equiv) was added dropwise (over 1.5 h). The mixture was stirred (additional 1 h), quenched with potassium phosphate monobasic (1 M aqueous, producing pH = 5), and extracted with EtOAc. The combined organic phase was washed with brine and dried with sodium sulfate. Volatiles were removed under reduced pressure and the crude material was purified via column chromatography.

*General Procedure for Syntheses of Allylic Chlorides (**4**, **5**, **16**, **22**, **24**)*. Lithium chloride was dried in a vacuum oven overnight. Into a flame-dried flask were added the required alcohol (1 equiv), lithium chloride (1.2 equiv), and toluene. Volatiles were removed under reduced pressure (to remove any residual water). The flask was capped with a rubber septum and maintained under a nitrogen atmosphere. To the flask were added DMF (0.3 M), 2,6-lutidine (4 equiv) and methanesulfonyl chloride (2 equiv). The mixture was stirred (4 h), quenched with sodium bicarbonate (50% saturated), extracted with hexane, washed with sodium bisulfate (1 M aqueous), washed with a 1:1 mixture of brine and 1 M aqueous sodium bisulfate, and dried with sodium sulfate. Volatiles were removed under reduced pressure to yield the crude product. In some cases, minor amounts of the isomeric tertiary chlorides, resulting from allylic substitution pathways, were also observed. The allylic chlorides are not fully stable to silica gel.

General Procedure for Measuring Kinetics of Reactions between Pyridine and Allylic Chlorides. The allylic chloride (approximately 25–60 mg) was added to a tared 1 dram vial and dissolved in the appropriate volume of $CDCl_3$ (typically 200–360 μL) to create a 0.83 M solution. Pyridine (approximately 55–110 mg) was added to a second tared 1 dram vial and dissolved in the appropriate volume of $CDCl_3$ (typically 0.9–1.7 mL) to give a 0.83 M solution. Into an NMR tube were combined 100 μL of the allylic chloride solutions and 300 μL of the pyridine solution (final concentrations 0.21 M = 1 equiv chloride and 0.63 M = 3 equiv pyridine). The tube was capped and mixed thoroughly, and the time of the mixing was recorded as time zero. All experiments were conducted at 23–24 °C, and each experiment was maintained in a +/- 0.5 °C range and compared to other runs performed simultaneously at the same temperature.

Formation of pyridinium products was monitored by ^1H NMR, specifically by the disappearance of the CH_2–Cl doublet and the formation of the CH_2–N doublet, except in the case

of THP-protected geranyl chloride **5**, whose CH_2–Cl doublet overlaps other signals, so conversion was monitored by the disappearance of the two vinyl triplets from the starting chloride and the formation of the CH_2–N doublet. NMR spectra of these reactions are provided in the supporting information. All rate comparisons were made using experiments that were performed simultaneously in side-by-side experiments. Any minor amounts of tertiary allylic chlorides present did not react under these conditions.

As a representative example, an aliquot of pyridinium chloride **9** (geranylpyridinium chloride) was isolated for characterization as a hydroscopic oil by removing the volatiles under reduced pressure (chloroform azeotrope).

*Chloride **4** ((2E,6E)-8-Chloro-1-tertbutyldimethylsiloxy-2,6-dimethyl-2,6-octadiene).* The general procedure was followed using alcohol **4B** (147 mg, 0.50 mmol, 1 equiv), LiCl (25 mg, 0.60 mmol, 1.2 equiv), toluene (5 mL), DMF (2.0 mL, 0.25 M), 2,6-lutidine (231 µL, 2.0 mmol, 4.0 equiv), MsCl (78 µL, 1.0 mmol, 2.0 equiv), hexane (3 x 5 mL), and aqueous washes (5 mL each). Crude chloride **4** (140 mg, 0.462 mmol, 89% crude yield, pale yellow oil), which is not completely stable to silica gel, was assessed to be >95% pure by NMR and was used directly in the subsequent experiments.

^{1}H NMR ($CDCl_3$, 600 MHz) δ 5.45 (t, J = 7.9 Hz, 1H, C=CH), 5.36 (t, J = 6.9 Hz, 1H, C=CH), 4.10 (d, J = 7.9 Hz, 2H, CH_2–Cl), 4.00 (s, 2H, CH_2–OTBS), 2.16 (q, J = 7.1 Hz, 2H, C=C–CH_2), 2.09 (t, J = 7.6 Hz, 2H, C=C–CH_2), 1.73 (s, 3H, CH_3), 1.59 (s, 3H, CH_3), 0.91 (s, 9H, Si–*t*Bu), 0.06 (s, 6H, 2 x Si–Me).

^{13}C NMR ($CDCl_3$, 150 MHz) δ 142.6, 135.2, 123.6, 120.8, 68.6, 41.1, 39.3, 26.1, 25.8, 18.6, 16.2, 13.4, -5.1.

IR (neat, cm^{-1}) 2930, 2859, 1665, 1250, 1113, 1065, 832, 775, 668.

MS calculated for $[C_{16}H_{31}OSiClNa]^+$, requires m/z = 325.17, found m/z = 325.1 (ESI).

HRMS (decomposes under ESI and EI conditions, analyzed as cation after loss of chloride and as pyridinium adduct) calculated for $[C_{16}H_{31}OSi]^+$, requires m/z = 267.2144, found m/z = 267.2137 (ESI); calculated for $[C_{21}H_{36}NOSi]^+$, requires m/z = 346.2566, found m/z = 346.2562 (ESI).

TLC (5:1) hexane/EtOAc, permanganate, R_f = 0.86.

*Ether **4A** ((2E,6E)-8-tertbutyldimethylsiloxy-3,7-dimethyl-2,6-octadienyl acetate).* Into a flask were added alcohol **12** (2.94 g, 13.9 mmol, 1 equiv), DCM (28 mL, 0.5 M), imidazole (1.37 g, 20.1 mmol, 1.5 equiv), and *t*-butyldimethylchlorosilane (2.60 g, 17.3 mmol, 1.25 equiv). The mixture was stirred (16 h), quenched with ammonium chloride (50% saturated, 60 mL), and diluted with DCM (60 mL). The organic phase was isolated, washed with sodium chloride (50% saturated aqueous, 60 mL), and dried with sodium sulfate. Volatiles were removed under reduced pressure, and the crude material was purified by column chromatography (75 mL silica gel, 7:1 hexane / EtOAc) to yield pure ether **4A** (3.85 g, 11.8 mmol, 85% yield, colorless oil).

^{1}H NMR ($CDCl_3$, 600 MHz) δ 5.36 (t, J = 7.0 Hz, 1H, C=CH), 5.35 (t, J = 7.0 Hz, 1H, C=CH), 4.58 (d, J = 7.0 Hz, 2H, CH_2–OAc), 4.00 (s, 2H, CH_2–OTBS), 2.15 (q, J = 7.4 Hz, 2H, C=C–CH_2), 2.09–2.06 (m, 2H, C=C–CH_2), 2.05 (s, 3H, Ac), 1.70 (s, 3H, CH_3), 1.59 (s, 3H, CH_3), 0.90 (s, 9H, Si–*t*Bu), 0.05 (s, 6H, 2 x Si–Me).

^{13}C NMR ($CDCl_3$, 150 MHz) δ 171.1, 142.0, 134.9, 123.7, 118.5, 68.6, 61.4, 39.3, 26.0, 25.8, 21.1, 18.5, 16.5, 13.5, -5.2.

IR (neat, cm^{-1}) 2937, 2861, 1740, 1227, 1064, 838, 777.

HRMS calculated for $[C_{18}H_{34}O_3SiNa]^+$, requires *m*/*z* = 349.2175, found *m*/*z* = 349.2169 (ESI).

TLC (7:1) hexane/EtOAc, permanganate, R_f = 0.61.

*Alcohol **4B** ((2E,6E)-8-tertbutyldimethylsiloxy-3,7-dimethyl-2,6-octadien-1-ol).* Into a flask were added acetate **4A** (3.85 g, 11.8 mmol, 1 equiv), MeOH (40 mL, 0.3 M), and potassium carbonate (490 mg, 3.55 mmol, 0.3 equiv). The mixture was stirred (20 h), quenched with potassium phosphate monobasic (1.0 M aqueous, 40 mL, producing pH 5.0), and approximately half of the volume was removed under reduced pressure. The remaining mixture was extracted with ethyl acetate (3 x 50 mL), and the combined organic phase was washed with sodium chloride (50% saturated aqueous, 60 mL) and dried with sodium sulfate. Volatiles were removed under reduced pressure, and the crude material was purified by column chromatography (100 mL silica gel, [6:1 to 2:1] hexane / EtOAc) to yield pure alcohol **4B** (2.97 g, 10.5 mmol, 89% yield, colorless oil).

^{1}H NMR ($CDCl_3$, 600 MHz) δ 5.42 (t, *J* = 6.7 Hz, 1H, C=CH), 5.36 (t, *J* = 7.0 Hz, 1H, C=CH), 4.15 (d, *J* = 6.7 Hz, 2H, CH_2–OH), 4.00 (s, 2H, CH_2–OTBS), 2.16 (q, *J* = 7.5 Hz, 2H, C=C–CH_2), 2.05 (t, *J* = 7.5 Hz, 2H, C=C–CH_2), 1.68 (s, 3H, CH_3), 1.59 (s, 3H, CH_3), 0.90 (s, 9H, Si-*t*Bu), 0.06 (s, 6H, 2 x Si–Me).

^{13}C NMR ($CDCl_3$, 150 MHz) δ 139.5, 134.8, 124.0, 123.7, 68.7, 59.4, 39.3, 26.1, 25.9, 18.6, 16.3, 13.6, -5.1.

IR (neat, cm^{-1}) 3341, 2937, 2855, 1254, 1066, 835, 774.

HRMS calculated for $[C_{16}H_{32}O_2SiNa]^+$, requires *m*/*z* = 307.2069, found *m*/*z* = 307.2065 (ESI).

TLC (6:1) hexane/EtOAc, permanganate, R_f = 0.29.

*Chloride **5** ((2E,6E)-8-Chloro-1-tetrahydropyranyloxy-2,6-dimethyl-2,6-octadiene).* The general procedure was followed using alcohol **5B** (160 mg, 0.600 mmol, 1 equiv), LiCl (30 mg, 0.72 mmol, 1.2 equiv), toluene (5 mL), DMF (2.4 mL, 0.25 M), 2,6-lutidine (277 µL, 2.4 mmol, 4.0 equiv), MsCl (93 µL, 1.2 mmol, 2.0 equiv), hexane (3 x 5 mL), and aqueous washes (5 mL each). Crude chloride **5** (142 mg, 0.520 mmol, 87% crude yield, pale yellow oil), which is not completely stable to silica gel, was assessed to be >95% pure by NMR and was used directly for the subsequent experiments.

^{1}H NMR ($CDCl_3$, 600 MHz) δ 5.45 (t, *J* = 7.8 Hz, 1H, C=CH), 5.40 (t, *J* = 6.9 Hz, 1H, C=CH), 4.60 (t, *J* = 3.6 Hz, 1H, O–CH–O), 4.10 (d, *J* = 11.8 Hz, 1H, CH_2–OTHP), 4.09 (d, *J* = 7.8 Hz, 2H, CH_2–Cl), 3.88 (ddd, J_1 = 11.2 Hz , J_2 = 8.1 Hz , J_3 = 2.9 Hz, 1H, CH_2–O), 3.85 (d, *J* = 11.8 Hz, 1H, CH_2–OTHP), 3.51 (dt, J_d = 11.2 Hz , J_t = 5.3 Hz, 1H, CH_2–O), 2.18 (q, *J* = 7.3 Hz, 2H, C=C–CH_2), 2.10 (t, *J* = 7.6 Hz, 2H, C=C–CH_2), 1.88–1.82 (m, 1H, CH_2), 1.74–1.69 (m, 1H, CH_2), 1.73 (s, 3H, CH_3), 1.66 (s, 3H, CH_3), 1.63–1.51 (m, 4H, 2 x CH_2).

^{13}C NMR ($CDCl_3$, 150 MHz) δ 142.4, 132.7, 126.8, 120.7, 97.6, 72.8, 62.2, 41.0, 39.1, 30.8, 26.0, 25.6, 19.6, 16.1, 14.1.

IR (neat, cm^{-1}) 2950, 2857, 1665, 1116, 1080, 1019, 908, 873, 671.

MS calculated for $[C_{15}H_{25}O_2ClNa]^+$, requires *m*/*z* = 295.14, found *m*/*z* = 295.1 (ESI).

HRMS (decomposes, analyzed as elimination product and as pyridinium adduct) calculated for $[C_{15}H_{24}O_2Na]^+$, requires *m*/*z* = 259.1674, found *m*/*z* = 259.1673 (ESI); calculated for $[C_{20}H_{30}NO_2]^+$, requires *m*/*z* = 316.2277, found *m*/*z* = 316.2274 (ESI).

TLC (3:1) hexane/EtOAc, permanganate, R_f = 0.61.

*Ether **5A** ((2E,6E)-8-tetrahydropyranyloxy-3,7-dimethyl-2,6-octadienyl acetate).* Into a flame-dried flask were added alcohol **12** (1.10 g, 5.19 mmol, 1 equiv) and DCM (8.6 mL, 0.6 M). The flask was capped with a rubber septum and maintained under a nitrogen atmosphere. To the flask were added pyridinium *para*-toluenesulfonate (390 mg, 1.56 mmol, 0.3 equiv) and dihydropyran (1.25 mL, 13.0 mmol, 2.5 equiv). The flask was fit with a reflux condenser. The mixture was warmed in an oil bath (40 ºC), stirred (17 h), diluted with sodium chloride (50% saturated aqueous, 15 mL), and extracted with ethyl acetate (2 x 15 mL). The combined organic phase was washed with sodium chloride (50% saturated aqueous, 30 mL) and dried with sodium sulfate. Volatiles were removed under reduced pressure and crude ether **5A** (1.57 g, quantitative mass recovery) was used directly in the next step. For analysis, an aliquot was partially purified by column chromatography (silica gel, 5:1 hexane / EtOAc) to yield material that was >90% pure by ^{1}H NMR.

^{1}H NMR ($CDCl_3$, 600 MHz) δ 5.41 (t, J = 6.9 Hz, 1H, vinyl), 5.35 (t, J = 7.2 Hz, 1H, vinyl), 4.60 (t, J = 3.5 Hz, 1H, O–CH–O), 4.59 (d, J = 7.3 Hz, 2H, CH_2–OAc), 4.10 (d, J = 11.5 Hz, 1H, CH_2–OTHP), 3.90–3.86 (m, 1H, CH_2–O), 3.85 (d, J = 11.5 Hz, 1H, CH_2–OTHP), 3.53–3.49 (m, 1H, CH_2–O), 2.18 (q, J = 7.2 Hz, 2H, CH_2–C=C), 2.09–2.05 (m, 2H, CH_2–C=C), 2.04 (s, 3H, Ac), 1.88–1.82 (m, 1H, THP), 1.71 (s, 3H, CH_3), 1.66 (s, 3H, CH_3), 1.74–1.50 (m, 5H, THP).

^{13}C NMR ($CDCl_3$, 150 MHz) δ 171.1, 141.9, 132.4, 127.1, 118.5, 97.4, 72.8, 62.1, 61.3, 39.1, 30.7, 25.9, 25.5, 21.1, 19.6, 16.5, 14.1.

IR (neat, cm^{-1}) 2938, 2862, 1738, 1232, 1022.

HRMS calculated for $[C_{17}H_{28}O_4Na]^+$, requires m/z = 319.1885, found m/z = 319.1880 (ESI).

TLC (3:1) hexane/EtOAc, permanganate, R_f = 0.57.

*Alcohol **5B** ((2E,6E)-8-tetrahydropyranyloxy-3,7-dimethyl-2,6-octadien-1-ol).* Into a flask was added crude acetate **5A** (5.19 mmol, 1 equiv), methanol (13 mL, 0.4 M), and potassium carbonate (220 mg, 1.59 mmol, 0.3 equiv). The mixture was stirred (5 h), quenched with potassium phosphate monobasic (1 M, 15 mL, producing pH = 5), and extracted with ethyl acetate (3 x 30 mL). The combined organic phase was washed with sodium chloride (50% saturated aqueous, 50 mL) and dried with sodium sulfate. Volatiles were removed, and the crude material was purified by column chromatography (40 mL silica gel, 5:2 hexane / EtOAc) to yield pure alcohol **5B** (920 mg, 3.62 mmol, 70% yield from alcohol **12**, colorless oil).

^{1}H NMR ($CDCl_3$, 600 MHz) δ 5.43–5.38 (m, 2H, 2 x vinyl), 4.61 (t, J = 3.5 Hz, 1H, O–CH–O), 4.14 (d, J = 6.8 Hz, 2H, CH_2–OH), 4.09 (d, J = 11.5 Hz, 1H, CH_2–OTHP), 3.89–3.85 (m, 1H, CH_2–O), 3.86 (d, J = 11.5 Hz, 1H, CH_2–OTHP), 3.53–3.49 (m, 1H, CH_2–O), 2.23–2.13 (m, 2H, CH_2–C=C), 2.08 (t, J = 7.4 Hz, 2H, CH_2–C=C), 1.87–1.81 (m, 1H, THP), 1.67 (s, 3H, CH_3), 1.66 (s, 3H, CH_3), 1.74–1.50 (m, 5H, THP).

^{13}C NMR ($CDCl_3$, 150 MHz) δ 138.6, 132.0, 127.8, 124.0, 96.9, 72.9, 62.0, 59.2, 39.1, 30.6, 25.8, 25.5, 19.4, 16.1, 14.1.

IR (neat, cm^{-1}) 3406, 2927, 2868, 1118, 1016.

HRMS calculated for $[C_{15}H_{26}O_3Na]^+$, requires m/z = 277.1780, found m/z = 277.1777 (ESI).

TLC (5:2) hexane/EtOAc, permanganate, R_f = 0.30.

*Ketone **7** ((2R,3S,4S,5S)-2-[(2E,6E)-8-tertbutyldimethylsiloxy-3,7-dimethyl-2,6-octadienyl]-4-isopropenyl-5-methoxymethoxy-3-{[(p-methoxyphenyl)methoxy]methyl}-2-methylcyclopentanone).* The general alkylation procedure was followed using ketone **2** (143 mg,

0.41 mmol, 1 equiv), geranyl chloride **4** (311 mg, 1.03 mmol, 2.5 equiv), toluene (15 mL), THF (0.21 mL, 2 M), sodium hexamethyldisilazide (1.0 M in THF, 0.62 mL, 0.62 mmol, 1.5 equiv), potassium phosphate (5 mL), EtOAc (3 x 4 mL), and brine (5 mL). The crude material was purified via column chromatography (16 mL silica gel, 6:1 hexane/EtOAc) to yield ketone **7** (91 mg, 0.15 mmol, 36% yield, colorless oil) as a mixture of epimers at the CH–OMOM stereocenter (6:1 *S* / *R*). ^{1}H NMR signals of the major diasteromer were assigned by ^{1}H–^{1}H COSY and by comparison to the starting materials. The minor diastereomer was identified by comparing its ^{1}H NMR signals to those of analogous ketone **6**. Stereochemistry of the major diasteromer was assigned by ^{1}H–^{1}H NOESY and by comparison to ketone **6**. No other stereoisomers, constitutional isomers, or double-alkylation products were observed by ^{1}H NMR.

Major Isomer (*S* stereochemistry at OMOM):

^{1}H NMR ($CDCl_3$, 600 MHz) δ 7.12 (d, J = 8.6 Hz, 2H, Ar), 6.83 (d, J = 8.6 Hz, 2H, Ar), 5.34 (t, J = 6.5 Hz, 1H, C=CH), 5.13 (t, J = 7.2 Hz, 1H, C=CH), 5.05 (brs, 2H, C=CH_2) 5.03 (d, J = 6.6 Hz, 1H, O–CH_2–O), 4.69 (d, J = 6.6 Hz, 1H, O–CH_2–O), 4.61 (d, J = 10.8 Hz, 1H, CH–OMOM), 4.30 (d, J = 11.6 Hz, 1H, CH_2–Ar), 4.19 (d, J = 11.6 Hz, 1H, CH_2–Ar), 3.98 (s, 2H, CH_2–OTBS), 3.79 (s, 3H, Ar–O–CH_3), 3.37 (s, 3H, O–CH_3), 3.28–3.26 (m, 2H, CH_2–OPMB), 2.94 (dd, J_1 = 10.8 Hz, J_2 = 7.5 Hz, 1H, CH–C=C), 2.34 (dd, J_1 = 14.3 Hz, J_2 = 8.9 Hz, 1H, C=C–CH_2), 2.16–2.11 (m, 3H, C=C–CH_2, CH–C–OPMB), 2.08–2.04 (m, 2H, C=C–CH_2), 1.95 (dd, J_1 = 14.3 Hz, J_2 = 6.4 Hz, 1H, C=C–CH_2), 1.79 (s, 3H, C=C–CH_3), 1.63 (s, 3H, C=C–CH_3), 1.59 (s, 3H, C=C–CH_3), 1.09 (s, 3H, CH_3), 0.90 (s, 9H, *t*–Bu), 0.05 (s, 6H, 2 x Si–CH_3).

^{13}C NMR ($CDCl_3$, 150 MHz) δ 219.5, 159.2, 141.6, 139.2, 134.7, 130.1, 129.1, 124.2, 118.8, 113.8, 111.6, 96.2, 73.0, 68.8, 67.2, 55.9, 55.4, 51.0, 49.4, 42.5, 39.9, 35.7, 26.3, 26.1, 22.9, 18.6, 16.8, 16.6, 13.6, –5.1.

IR (neat, cm^{-1}) 3088, 2965, 2931, 2855, 1744, 1618, 1517, 1249, 1102, 1027, 835, 779.

HRMS calculated for $[C_{36}H_{58}O_6SiNa]^+$, requires m/z = 637.3900, found m/z = 637.3904 (ESI).

TLC (5:1) hexane / EtOAc, permanganate, R_f = 0.43.

Minor Isomer (*R* stereochemistry at OMOM):

^{1}H NMR ($CDCl_3$, 600 MHz, partially reported, nonoverlapping signals) δ 7.25 (d, J = 8.0 Hz, 2H, Ar), 6.88 (d, J = 8.1 Hz, 2H, Ar), 4.72 (d, J = 6.9 Hz, 1H, O–CH_2–O), 4.45 (d, J = 11.6 Hz, 1H, CH_2–Ar), 4.39 (d, J = 11.9 Hz, 1H, CH_2–Ar), 4.24 (d, J = 7.2 Hz, 1H, CH–OMOM), 3.99 (s, 2H, CH_2–OTBS), 3.51 (d, J = 6.9 Hz, 2H, CH_2–OPMB), 3.36 (s, 3H, O–CH_3), 2.54 (q, J = 7.0 Hz, 1H, CH–C–OPMB), 1.73 (s, 3H, C=C–CH_3), 1.57 (s, 3H, C=C–CH_3).

TLC (5:1) hexane / EtOAc, permanganate, R_f = 0.37.

*Ketone **8** ((2R,3S,4S,5S)-2-[(2E,6E)-8-tetrahydropyranyloxy-3,7-dimethyl-2,6-octadienyl]-4-isopropenyl-5-methoxymethoxy-3-{[(p-methoxyphenyl)methoxy]methyl}-2-methylcyclopentanone).*The general alkylation procedure was followed using ketone **2** (147 mg, 0.42 mmol, 1 equiv), geranyl chloride **5** (287 mg, 1.05 mmol, 2.5 equiv), toluene (15 mL), THF (0.21 mL, 2 M) sodium hexamethyldisilazide (1.0 M in THF, 0.63 mL, 0.63 mmol, 1.5 equiv), potassium phosphate (5 mL), EtOAc (3 x 4 mL), and brine (5 mL). The crude material was purified via column chromatography (20 mL silica gel, 5:1 hexane / EtOAc) to yield ketone **8** (60 mg, 0.10 mmol, 24% yield, colorless oil) as predominantly a single epimer at the CH–OMOM stereocenter. Analysis by ^{13}C NMR shows an approximate 1:1 mixture of diastereomers at the THP group. ^{1}H NMR signals were assigned by ^{1}H–^{1}H COSY and comparison to the

starting materials. Stereochemistry was assigned by ^{1}H–^{1}H NOESY and by comparison to ketone **6**.

^{1}H NMR ($CDCl_3$, 600 MHz, two diastereomers at THP) δ 7.12 (d, J = 8.6 Hz, 2H, Ar), 6.83 (d, J = 8.6 Hz, 2H, Ar), 5.39 (t, J = 6.6 Hz, 1H, C=CH), 5.12 (t, J = 7.4 Hz, 1H, C=CH), 5.04 (brs, 2H, C=CH_2), 5.02 (d, J = 6.9 Hz, 1H, O–CH_2–O), 4.69 (d, J = 6.9 Hz, 1H, O–CH_2–O), 4.61 (d, J = 10.7 Hz, 1H, CH–OMOM), 4.58 (t, J = 3.4 Hz, 1H, O–CH–O), 4.30 (d, J = 11.6 Hz, 1H, CH_2–Ar), 4.19 (d, J = 11.6 Hz, 1H, CH_2–Ar), 4.08 (d, J = 11.6 Hz, 1H, CH_2–OTHP), 3.88–3.85 (m, 1H, CH_2–O), 3.82 (d, J = 11.6 Hz, 1H, CH_2–OTHP), 3.79 (s, 3H, Ar–O–CH_3) 3.51–3.48 (m, 1H, CH_2–O), 3.37 (s, 3H, O–CH_3), 3.27 (brs, 2H, CH_2–OPMB), 2.94 (dd, J_1 = 10.7 Hz, J_2 = 7.6 Hz, 1H, CH–C=C), 2.33 (dd, J_1 = 14.5 Hz, J_2 = 8.9 Hz, 1H, C=C–CH_2), 2.17–2.12 (m, 3H, C=C–CH_2, CH–C–OPMB), 2.09–2.06 (m, 2H, C=C–CH_2), 1.96 (dd, J_1 = 14.5 Hz, J_2 = 6.1 Hz, 1H, C=C–CH_2), 1.86–1.75 (m, 1H, THP), 1.79 (s, 3H, C=C–CH_3), 1.73–1.67 (m, 1H, THP), 1.65 (s, 3H, C=C–CH_3), 1.63 (s, 3H, C=C–CH_3), 1.62–1.50 (m, 4H, THP), 1.08 (s, 3H, CH_3).

^{13}C NMR ($CDCl_3$, 150 MHz, two diastereomers at THP) δ 219.4, 159.2, 141.5, 139.0, 132.3, 130.1, 129.1, 127.5, 127.5, 119.0, 118.9, 113.8, 111.6, 97.6, 97.5, 96.1, 73.0, 67.2, 62.3, 55.8, 55.3, 51.0, 49.4, 42.5, 39.8, 35.7, 30.8, 26.4, 26.4, 25.6, 22.9, 19.6, 16.8, 16.6, 16.5, 14.2.

IR (neat, cm^{-1}) 3088, 2941, 2860, 1749, 1613, 1517, 1441, 1254, 1102, 1027, 820.

HRMS calculated for $[C_{35}H_{52}O_7Na]^+$, requires m/z = 607.3611, found m/z = 607.3616 (ESI).

TLC (5:1) hexane / EtOAc, permanganate, R_f = 0.31.

Formation of pyridinium **9** from geranyl chloride was monitored by ^{1}H NMR, specifically by the disappearance of the CH_2–Cl doublet and the formation of the CH_2–N doublet. For characterization, an aliquot of the crude reaction product was isolated as a hydroscopic oil by removing the volatiles under reduced pressure (chloroform azeotrope). ^{1}H NMR signals were assigned by ^{1}H–^{1}H COSY.

^{1}H NMR ($CDCl_3$ with 0.6 M pyridine, 600 MHz) δ 9.36 (brs, 2H, py), 8.42 (t, J = 7.4 Hz, 1H, py), 8.04 (t, J = 7.4 Hz, 2H, py), 5.52 (d, J = 7.5 Hz, 2H, CH_2–py), 5.40 (t, J = 7.5 Hz, 1H, CH=C), 4.88 (brs, 1H, CH=C), 1.99 (brs, 4H, 2 x CH_2), 1.77 (s, 3H, CH_3), 1.51 (s, 3H, CH_3), 1.44 (s, 3H, CH_3).

^{1}H NMR ($CDCl_3$, 600 MHz, after isolation) δ 9.46 (d, J = 5.3 Hz, 2H, py), 8.49 (t, J = 7.4 Hz, 1H, py), 8.10 (t, J = 6.9 Hz, 2H, py), 5.67 (d, J = 7.4 Hz, 2H, CH_2–py), 5.49 (t, J = 7.4 Hz, 1H, CH=C), 5.03–4.98 (brs, 1H, CH=C), 2.15–2.08 (brs, 4H, 2 x CH_2), 1.88 (s, 3H, CH_3), 1.64 (s, 3H, CH_3), 1.56 (s, 3H, CH_3).

^{13}C NMR ($CDCl_3$, 150 MHz, after isolation) δ 148.7, 145.1, 144.9, 132.6, 128.4, 123.2, 115.9, 59.4, 39.6, 26.1, 25.8, 17.9, 17.3.

IR (neat, cm^{-1}) 3387, 3063, 2978, 2924, 2861, 1635, 1490, 1154, 776, 682.

HRMS calculated for $[C_{15}H_{22}N]^+$, requires m/z = 216.1752, found m/z = 216.1751 (ESI).

Formation of pyridinium **10** from chloride **4** was monitored by ^{1}H NMR, specifically by the disappearance of the CH_2–Cl doublet and the formation of the CH_2–N doublet.

^{1}H NMR ($CDCl_3$ with 0.6 M pyridine, 600 MHz) δ 9.38 (brs, 2H, py), 8.40 (t, J = 7.2 Hz, 1H, py), 8.04 (t, J = 7.2 Hz, 2H, py), 5.54 (d, J = 7.2 Hz, 2H, CH_2–py), 5.42 (t, J = 7.2 Hz, 1H, C=CH), 5.21 (brs, 1H, C=CH), 3.86 (s, 2H, CH_2–OTBS), 2.04 (brs, 4H, 2 x C=C–CH_2), 1.79 (s, 3H, CH_3), 1.45 (s, 3H, CH_3), 0.78 (s, 9H, Si–*t*Bu), -0.07 (s, 6H, 2 x Si–Me).

HRMS calculated for $[C_{21}H_{36}NOSi]^+$, requires m/z = 346.2566, found m/z = 346.2562 (ESI).

Formation of pyridinium **11** from chloride **5** was monitored by ^{1}H NMR. Since the CH_2–Cl doublet overlaps other signals, conversion was monitored by the disappearance of the two vinyl triplets from the starting chloride and the formation of the CH_2–N doublet.

^{1}H NMR ($CDCl_3$ with 0.6 M pyridine, 600 MHz) δ 9.36 (brs, 2H, py), 8.39 (t, J = 7.2 Hz, 1H, py), 8.03 (t, J = 7.2 Hz, 2H, py), 5.52 (d, J = 7.2 Hz, 2H, CH_2–py), 5.40 (t, J = 7.2 Hz, 1H, C=CH), 5.21 (brs, 1H, C=CH), 4.42 (brs, 1H, O–CH–O), 3.93 (d, J = 11.6 Hz, 1H, CH_2–OTHP), 3.76–3.70 (m, 1H, CH_2–O), 3.67 (d, J = 11.6 Hz, 1H, CH_2–OTHP), 3.38–3.30 (m, 1H, CH_2–O), 2.04 (brs, 4H, 2 x C=C–CH_2), 1.77 (s, 3H, CH_3), 1.72–1.31 (m, 6H, 3 x CH_2), 1.50 (s, 3H, CH_3).

HRMS calculated for $[C_{20}H_{30}NO_2]^+$, requires m/z = 316.2277, found m/z = 316.2274 (ESI).

*Bromide **13** ((2E,6E)-8-Bromo-3,7-dimethyl-2,6-octadienyl acetate)*. A flame-dried flask was capped with a rubber septum and maintained under a nitrogen atmosphere. Into the flask were added alcohol **12** (500 mg, 2.36 mmol, 1 equiv) and DCM (6.0 mL 0.4 M). The flask was cooled in an ice bath (0 °C). Into the flask were added 2,6-lutidine (820 µL, 7.08 mmol, 3.0 equiv), tetrabutylammonium bromide (1.96 g, 5.90 mmol, 2.5 equiv), and methanesulfonic anhydride (615 mg, 3.54 mmol, 1.5 equiv). The mixture was stirred (4 h), allowed to warm to ambient temperature, quenched with water (10 mL), and extracted with pentane (3 x 15 mL). The combined organic phase was washed with sodium bisulfate (1 M aqueous, 20 mL), washed with a 1:1 mixture of brine and 1 M aqueous sodium bisulfate (25 mL), and dried with sodium sulfate. Volatiles were removed under reduced pressure to yield crude bromide **13** (654 mg, brown oil, quantitative mass recovery, mostly pure by ^{1}H NMR), which was used directly in the next step. Bromide **13** is not fully stable to silica gel.

^{1}H NMR ($CDCl_3$, 600 MHz) δ 5.57 (t, J = 6.9 Hz, 1H, HC=C), 5.34 (t, J = 6.9 Hz, 1H, HC=C), 4.59 (d, J = 6.9 Hz, 2H, CH_2–OAc), 3.96 (s, 2H, CH_2–Br), 2.17 (q, J = 6.9 Hz, 2H, C=C–CH_2), 2.09 (t, J = 7.4 Hz, 2H, C=C–CH_2), 2.06 (s, 3H, Ac), 1.76 (s, 3H, CH_3), 1.70 (s, 3H, CH_3).

^{13}C NMR ($CDCl_3$, 150 MHz) δ 170.9, 141.2, 132.5, 130.4, 119.0, 61.2, 41.5, 38.6, 26.4, 21.0, 16.4, 14.7.

IR (neat, cm^{-1}) 3023, 2934, 2857, 1733, 1667, 1445, 1364, 1233, 1022, 949, 604.

MS calculated for $[C_{12}H_{19}O_2BrNa]^+$, requires m/z = 297.05 and 299.04, found m/z = 297.1 and 299.1 (ESI).

HRMS (decomposes under ESI and EI conditions, analyzed as symmetric ether dimer) calculated for $[C_{24}H_{38}O_5Na]^+$, requires m/z = 429.2617, found m/z = 429.2610 (ESI).

TLC (4:1) hexane/EtOAc, permanganate, R_f = 0.59.

*Sulfone **14** (**(Ethylsulfonyl)benzene)*. A flame-dried flask was capped with a rubber septum and maintained under a nitrogen atmosphere. Into the flask were added sodium benzenesulfinate (5.79 g, 35.3 mmol, 1.4 equiv), DMF (5 mL, 5 M), and iodoethane (2.05 mL, 25.6 mmol, 1 equiv). The mixture was stirred (24 h), diluted with sodium chloride (50% saturated aqueous, 10 mL), and extracted with Et_2O (3 x 10 mL). The combined organic phase was washed with sodium chloride (50% saturated aqueous, 20 mL) and dried with sodium sulfate. Volatiles were removed under reduced pressure, and the crude material was purified by column chromatography (60 mL silica gel, 3:1 hexane / EtOAc) to yield pure sulfone **14** (3.84 g, 22.6 mmol, 88% yield, colorless solid). ^{1}H NMR analysis is consistent with previously reported data.[32]

^{1}H NMR ($CDCl_3$, 200 MHz) δ 7.91 (d, J = 7.6 Hz, 2H, Ar), 7.74–7.47 (m, 3H, Ar), 3.12 (q, J = 7.6 Hz, 2H, CH_2), 1.27 (t, J = 7.7 Hz, 3H, CH_3).

*Sulfone **15** ((2E,6E)-3,7-Dimethyl-9-(phenylsulfonyl)-2,6-decadien-1-ol)*. A flame-dried flask was capped with a rubber septum and maintained under a nitrogen atmosphere. Into the flask were added ethyl phenyl sulfone (**14**, 1.61 g, 9.44 mmol, 4 equiv) and THF (9.5 mL). The flask was cooled in an ice bath (0 °C). To the mixture were added KHMDS (0.5 M in toluene, 14.2 mL, 7.08 mmol, 3.0 equiv). The mixture was stirred (30 min). Bromide **13** (654 mg, 2.36 mmol, 1 equiv) was dissolved in THF (5.0 mL) and added dropwise to the flask (final concentration 0.08 M). The reaction was stirred (3 h), quenched with potassium phosphate monobasic (1 M aqueous, 30 mL, producing pH = 5), allowed to warm to ambient temperature, and extracted with EtOAc (3 x 30 mL). The combined organic phase was washed with sodium chloride (50% saturated aqueous, 50 mL) and dried with sodium sulfate. Volatiles were removed under reduced pressure, and the crude material was purified by column chromatography (45 mL silica gel, [2:1 to 3:2] hexane / EtOAc) to yield pure sulfone **15** (129 mg) plus mixed fractions (containing material in which the acetate appeared to not yet have been removed). The mixed fractions were combined with methanol (1.5 mL) and potassium carbonate (26 mg), stirred at ambient temperature (1 h), worked up as described above, and purified by silica gel chromatography to yield pure sulfone **15** (375 mg total, 1.16 mmol, 49% yield, colorless oil).

^{1}H NMR ($CDCl_3$, 600 MHz) δ 7.89 (d, J = 7.4 Hz, 2H, Ar), 7.66 (t, J = 7.4 Hz, 1H, Ar), 7.57 (t, J = 7.4 Hz, 2H, Ar), 5.38 (t, J = 6.6 Hz, 1H, HC=C), 5.15 (t, J = 6.3 Hz, 1H, HC=C), 4.13 (d, J = 6.6 Hz, 2H, CH_2–O), 3.18–3.12 (m, 1H, CH), 2.68 (d, J = 12.4 Hz, 1H, CH_2–C–S), 2.11 (q, J = 7.0 Hz, 2H, CH_2–C=C). 2.05–1.99 (m, 3H, C=C–CH_2, CH_2–C–S), 1.65 (s, 3H, CH_3), 1.52 (s, 3H, CH_3), 1.16 (d, J = 6.8 Hz, 3H, CH_3).

^{13}C NMR ($CDCl_3$, 150 MHz) δ 138.7, 137.2, 133.7, 129.9, 129.1, 129.0, 128.7, 123.9, 59.2, 58.2, 39.3, 39.1, 26.2, 16.2, 15.5, 12.7.

IR (neat, cm^{-1}) 3446, 3070, 2980, 2920, 2857, 1444, 1299, 1146, 1090, 1004, 732, 691.

HRMS calculated for $[C_{18}H_{26}O_3SNa]^+$, requires m/z = 345.1500, found m/z = 345.1497 (ESI).

TLC (1:1) hexane/EtOAc, UV/permanganate, R_f = 0.38.

*Alcohol **15A** ((2E,6E)-3,7-Dimethyl-2,6-decadien-1-ol).* A flame-dried flask was capped with a rubber septum and maintained under a nitrogen atmosphere. Into the flask were added sulfone **15** (246 mg, 0.764 mmol, 1 equiv) and MeOH (distilled from Na_2SO_4, 7.6 mL, 0.1 M). The flask was cooled in an ice bath (0 °C). Sodium mercury amalgam (20% Na, 1.76 g, 15.2 mmol, 20.0 equiv) was added. The mixture was stirred (4 h, gradually warming to ambient temperature) diluted with Et_2O (20 mL), and washed with water (20 mL). Insolubles were removed from the organic phase by gravity filtration and chased with Et_2O (20 mL). The combined organic phase was dried with sodium sulfate. Volatiles were gently removed under reduced pressure, and the crude material was purified by column chromatography (20 mL silica, 2:1 pentane/Et_2O) to yield pure alcohol **15A** (94 mg, 0.52 mmol, 68% yield, volatile colorless oil).

^{1}H NMR ($CDCl_3$, 600 MHz) δ 5.42 (t, J = 6.5 Hz, 1H, C=CH), 5.09 (t, J = 6.4 Hz, 1H, C=CH), 4.15 (d, J = 6.5 Hz, 2H, CH_2–OH), 2.12 (q, J = 6.9 Hz, 2H, C=C–CH_2), 2.05 (t, J = 7.8 Hz , 2H, C=C–CH_2), 1.94 (t, J = 7.3 Hz, 2H, C=C–CH_2), 1.68 (s, 3H, CH_3), 1.58 (s, 3H, CH_3), 1.40 (sext, J = 7.3 Hz, 2H, CH_2), 1.24 (brs, 1H, OH), 0.86 (t, J = 7.3 Hz, 3H, CH_3).

^{13}C NMR ($CDCl_3$, 150 MHz) δ 139.9, 135.6, 123.9, 123.5, 59.5, 41.9, 39.7, 26.4, 21.1, 16.4, 16.0, 13.8.

IR (neat, cm^{-1}) 3314, 3052, 2962, 2927, 2869, 1670, 1447, 1380, 1002.

HRMS calculated for $[C_{12}H_{22}O]^+$, requires *m*/*z* = 182.1671, found *m*/*z* = 182.1679 (EI)..
TLC (2:1) hexane/EtOAc, permanganate, R_f = 0.58.

*Chloride **16** ((2E,6E)-1-Chloro-3,7-dimethyl-2,6-decadiene).* The general procedure was followed using alcohol **15A** (94 mg, 0.52 mmol, 1 equiv), LiCl (26 mg, 0.62 mmol, 1.2 equiv), no toluene azeotrope due to alcohol **15A**'s volatility, DMF (2.1 mL, 0.25 M), 2,6-lutidine (240 µL, 2.08 mmol, 4.0 equiv), MsCl (96 µL, 1.2 mmol, 2.0 equiv), hexane (3 x 5 mL), and aqueous washes (5 mL each). Crude chloride **16** (89 mg, 0.44 mmol, 85% crude yield, pale yellow oil), which is not completely stable to silica gel, was assessed to be approximately 90% pure by NMR and was used directly for the subsequent experiments.

^{1}H NMR ($CDCl_3$, 600 MHz) δ 5.44 (t, *J* = 7.7 Hz, 1H, C=CH), 5.08 (t, *J* = 6.5 Hz, 1H, C=CH), 4.09 (d, *J* = 7.7 Hz, 2H, CH_2–Cl), 2.12 (q, *J* = 7.2 Hz, 2H, C=C–CH_2), 2.07 (t, *J* = 6.8 Hz, 2H, C=C–CH_2), 1.94 (t, *J* = 7.3 Hz, 2H, C=C–CH_2), 1.73 (s, 3H, CH_3), 1.58 (s, 3H, CH_3), 1.40 (sext, *J* = 7.3 Hz, 2H, CH_2), 0.85 (t, *J* = 7.3 Hz, 3H, CH_3).

^{13}C NMR ($CDCl_3$, 150 MHz) δ 142.9, 135.8, 123.6, 120.5, 41.9, 41.3, 39.6, 26.2, 21.1, 16.2, 16.0, 13.8.

IR (neat, cm^{-1}) 3057, 2962, 2931, 2874, 1668, 1455, 1383, 1254, 878, 674.

MS (decomposes under ESI conditions)

HRMS (decomposes under ESI conditions, analyzed as pyridinium adduct) calculated for $[C_{17}H_{26}N]^+$, requires *m*/*z* = 244.2065, found *m*/*z* = 244.2063 (ESI).

TLC (5:1) hexane/EtOAc, permanganate, R_f = 0.81.

Formation of pyridinium **16A** from chloride **16** was monitored by ^{1}H NMR, specifically by the disappearance of the CH_2–Cl doublet and the formation of the CH_2–N doublet.

^{1}H NMR ($CDCl_3$ with 0.6 M pyridine, 600 MHz) δ 9.43 (brs, 2H, py), 8.43 (t, *J* = 7.1 Hz, 1H, py), 8.04 (t, *J* = 7.1 Hz, 2H, py), 5.56 (d, *J* = 7.2 Hz, 2H, CH_2–py), 5.42 (t, *J* = 7.2 Hz, 1H, C=CH), 4.91 (brs, 1H, C=CH), 2.02 (brs, 4H, 2 x C=C–CH_2), 1.83–1.76 (m, 5H, CH_3, C=C–CH_2), 1.43 (s, 3H, CH_3), 1.24 (sext, *J* = 7.1 Hz, 2H, CH_2), 0.71 (t, *J* = 7.1 Hz, 3H, CH_3).

HRMS calculated for $[C_{17}H_{26}N]^+$, requires *m*/*z* = 244.2065, found *m*/*z* = 244.2063 (ESI).

*Ketone **19** (6-Methyl-2-heptanone).* Nickel (II) chloride hexahydrate (9.80 g, 41.2 mmol, 0.4 equiv) was heated under vacuum with a Bunsen burner (changing from green to yellow). Granular zinc (14.0 g, 213 mmol, 2.2 equiv) was added, and the flask was capped with a rubber septum and maintained under an argon atmosphere. To the flask were added THF (100 mL), pyridine (50 mL, producing a teal-color), and methyl vinyl ketone (**17**, 16.0 mL, 192 mmol, 2 equiv). The mixture was heated to reflux (1.5 h, producing a blood-red colored solution) and allowed to cool to ambient temperature. To the mixture was added 1-iodo-2-methylpropane (**18**, 11.3 mL, 98.2 mmol, 1 equiv). The mixture was stirred at ambient temperature (30 min), heated to reflux (16 h), cooled to ambient temperature, diluted with DCM (100 mL), filtered through a plug of Celite, washed with hydrochloric acid (1 M aqueous, 2 x 125 mL), washed with sodium bicarbonate (saturated aqueous, 2 x 125 mL), washed with sodium chloride (saturated aqueous, 125 mL), and dried with sodium sulfate. Volatiles were gently removed under reduced pressure (35 °C, 350–450 mbar). The crude material (33.0 g) was washed with hydrochloric acid (1 M aqueous, 2 x 100 mL) and sodium chloride (50% saturated aqueous, 100 mL). Volatiles were again removed under reduced pressure (35 °C, 350–450 mbar). The crude material (12.7 g) was purified via column chromatography (300 mL silica gel, 20:1 DCM / Et_2O). After volatiles were

gently removed, ketone **19** was isolated along with residual DCM (3.27 g, 66% ketone by mass, 16.9 mmol, 17% yield, colorless liquid). ^{1}H NMR analysis is consistent with commercially available material.

^{1}H NMR ($CDCl_3$, 200 MHz) δ 2.41 (t, J = 7.5 Hz, 2H, CH_2–C=O), 2.14 (s, 3H, CH_3–C=O), 1.67–1.44 (m, 3H, CH, CH_2), 1.22–1.10 (m, 2H, CH_2), 0.88 (d, J = 6.6 Hz, 6H, 2 x CH_3).

TLC (20:1) DCM/diethyl ether, dinitrophenylhydrazine, R_f = 0.86.

*Phosphonate Ester **20** (ethyl (diethoxyphosphinyl)acetate).* Into a flask were added ethyl bromoacetate (6.62 mL, 60.0 mmol, 1 equiv) and triethyl phosphite (25.6 mL, 150 mmol, 2.5 equiv). The mixture was heated to reflux (22 h), allowed to cool to ambient temperature, and distilled under reduced pressure (0.3 torr) to yield phosphonate ester **20** (11.6 g, 51.8 mmol, 86% yield, colorless liquid). ^{1}H NMR analysis is consistent with commercially available material.

^{1}H NMR ($CDCl_3$, 200 MHz) δ 4.22–4.03 (m, 6H, 3 x O–CH_2), 2.91 (d, J = 21.6 Hz, 2H, CH_2), 1.30 (t, J = 7.1, 6H, 2 x CH_3), 1.24 (t, J = 7.1, 3H, CH_3).

B.P. 160–165 °C (0.3 torr)

*Ester **21** (Ethyl (E)-3,7-dimethyl-2-octenoate).* Into a flame-dried flask were added sodium hydride (60% dispersion in mineral oil, 1.07 g, 26.8 mmol, 2.0 equiv) and THF (100 mL). The flask was capped with a rubber septum, maintained under a nitrogen atmosphere, and cooled in an ice bath (0 °C). Phosphonate ester **20** (6.60 g, 29.5 mmol, 2.2 equiv) was added dropwise (producing gas evolution). The mixture was stirred (30 min, until gas evolution ceased). Ketone **19** (1.71 g, 13.4 mmol, 1 equiv) was dissolved in THF (50 mL) and added to the reaction mixture (final concentration 0.09 M). The mixture was stirred (75 min), allowed to warm to ambient temperature, stirred (additional 17 h), diluted with DCM (100 mL), and quenched with sodium chloride (50% saturated aqueous, 150 mL). The organic phase was isolated, washed with sodium chloride (50% saturated aqueous, 2 x 100 mL), and dried with sodium sulfate. Volatiles were removed under reduced pressure. Analysis of the crude material by ^{1}H NMR showed a 4:1 ratio of *E* and *Z* isomers. The crude mixture was purified via column chromatography (80 mL silica gel, 10:1 DCM / Et_2O) yield ester **21-E** (737 mg, 3.72 mmol, 28% yield, colorless oil), ester **21-Z** (92 mg, 0.46 mmol, 3% yield, colorless oil), and a mixture of the two (918 mg, 4.63 mmol, 35% yield, colorless oil). ^{1}H NMR analysis is consistent with previously reported data.[33,34] *E* and *Z* isomers were assigned by comparison to previously reported data for **21-E**[33] and for analogous ***Z***-compounds.[35]

Major isomer (*E*).

^{1}H NMR ($CDCl_3$, 600 MHz) δ 5.65 (brs, 1H, C=CH), 4.14 (q, J = 7.2 Hz, 2H, CH_2–O), 2.15 (s, 3H, C=C–CH_3), 2.11 (t, J = 7.7 Hz, 2H, C=C–CH_2), 1.54 (non, J = 6.7 Hz, 1H, CH), 1.47 (pent, J = 7.7 Hz, 2H, CH_2), 1.28 (t, J = 7.2 Hz, 3H, CH_3), 1.18–1.13 (m, 2H, CH_2), 0.87 (d, J = 6.9 Hz, 6H, 2 x CH_3).

^{13}C NMR ($CDCl_3$, 50 MHz) δ 167.0, 160.4, 115.6, 59.5, 41.3, 38.6, 28.0, 25.3, 22.7, 18.8, 14.5.

IR (neat, cm^{-1}) 2956, 1715, 1648, 1221, 1148, 1118, 1042.

MS calculated for $[C_{12}H_{22}O_2Na]^+$, requires m/z = 221.15, found m/z = 221.2 (ESI).

TLC (15:1) hexane/Et_2O, permanganate, R_f = 0.42.

Minor Isomer (*Z*)

^{1}H NMR ($CDCl_3$, 200 MHz) δ 5.65 (brs, 1H, C=CH), 4.14 (q, J = 7.1 Hz, 2H, CH_2–O), 2.60 (t, J = 7.7 Hz, 2H, C=C–CH_2), 1.88 (d, J = 1.3 Hz, 3H, C=C–CH_3), 1.69–1.33 (m, 3H, CH, CH_2), 1.29–1.16 (m, 2H, CH_2), 1.27 (t, J = 7.1 Hz, 3H, CH_3), 0.88 (d, J = 6.5 Hz, 6H, CH_3).

TLC (15:1) hexane/Et_2O, permanganate, R_f = 0.50.

*Alcohol **21A** ((E)-3,7-Dimethyl-2-octen-1-ol)*. Into a flame-dried flask were added ester **21** (145 mg, 0.732 mmol, 1 equiv, pure *E*-isomer) and DCM (2.4 mL, 0.3 M). The flask was capped with a rubber septum, maintained under a nitrogen atmosphere, and cooled in an EtOAc/N_2(l) bath (-84 °C). DiBAl–H (1 M in hexane, 2.2 mL, 2.2 mmol, 3.0 equiv) was added, and the reaction was stirred (1 h), quenched with MeOH (2 mL) and then sodium hydroxide (1 M aqueous, 3 mL), allowed to warm to ambient temperature, diluted with water (3 mL) extracted with Et_2O (3 x 5 mL), washed with brine (5 mL), and dried with sodium sulfate. Volatiles were gently removed under reduced pressure, and the crude material was purified by column chromatography (16 mL silica gel, 3:1 hexane / Et_2O) to yield pure alcohol **21A** (97 mg, 0.62 mmol, 85% yield, slightly volatile colorless oil). ^{1}H NMR analysis is consistent with previously reported data.[34]

^{1}H NMR ($CDCl_3$, 600 MHz) δ 5.41 (t, J = 6.6 Hz, 1H, C=CH), 4.14 (d, J = 6.3 Hz, 2H, CH_2–O), 1.99 (t, J = 7.7 Hz, 2H, C=C–CH_2), 1.67 (s, 3H, CH_3), 1.53 (non, J = 6.7 Hz, 1H, CH), 1.40 (pent, J = 7.7 Hz, 2H, CH_2), 1.20 (d, J = 10.6 Hz, 1H, OH), 1.17–1.12 (m, 2H, CH_2), 0.87 (d, J = 6.7 Hz, 6H, CH_3).

^{13}C NMR ($CDCl_3$, 150 MHz) δ 140.2, 123.2, 59.5, 39.9, 38.7, 28.0, 25.6, 22.7, 16.3.

IR (neat, cm^{-1}) 3322, 2953, 2927, 2873, 1675, 1470, 1383, 1368, 999.

MS calculated for $[C_{10}H_{20}ONa]^+$, requires m/z = 179.14, found m/z = 179.2 (ESI).

TLC (3:1) hexane/Et_2O, permanganate, R_f = 0.30.

*Chloride **22** ((E)-1-Chloro-3,7-dimethyl-2-octene)*. The general procedure was followed using alcohol **21A** (170 mg, 1.09 mmol, 1 equiv), LiCl (55 mg, 1.3 mmol, 1.2 equiv), no toluene azeotrope due to alcohol **21A**'s volatility, DMF (4.3 mL, 0.25 M), 2,6-lutidine (315 µL, 2.72 mmol, 2.5 equiv), MsCl (169 µL, 2,18 mmol, 2.0 equiv), hexane (8 + 2 x 4 mL), and aqueous washes (5 mL each). Crude chloride **22** (172 mg, 0.98 mmol, 90% crude yield, pale yellow oil), which is not completely stable to silica gel, was assessed to be approximately 95% pure by NMR and was used directly for the subsequent experiments. ^{1}H NMR signals were assigned by ^{1}H–^{1}H COSY and by comparison to signals from the starting materials.

^{1}H NMR ($CDCl_3$, 600 MHz) δ 5.44 (t, J = 7.5 Hz, 1H, C=CH), 4.10 (d, J = 7.5 Hz, 2H, CH_2–Cl), 2.01 (t, J = 7.6 Hz, 2H, C=C–CH_2), 1.71 (s, 3H, C=C–CH_3), 1.53 (non, J = 6.7 Hz, 1H, CH), 1.43–1.38 (m, 2H, CH_2), 1.14 (dt, J_d = 7.6 Hz, J_t = 6.7 Hz, 2H, CH_2), 0.87 (d, J = 6.7 Hz, 6H, 2 x CH_3).

^{13}C NMR ($CDCl_3$, 150 MHz) δ 143.5, 120.1, 41.4, 39.8, 38.6, 28.0, 25.4, 22.8, 16.1.

IR (neat, cm^{-1}) 2961, 2937, 2867, 1666, 1464, 1385, 1254, 674.

MS (decomposes under ESI conditions)

HRMS (decomposes under ESI conditions, analyzed as pyridinium adduct) calculated for $[C_{15}H_{24}N]^+$, requires m/z = 218.1909, found m/z = 218.1907 (ESI).

TLC (5:1) hexane/EtOAc, permanganate, R_f = 0.90.

Formation of pyridinium **22A** from chloride **22** was monitored by ^{1}H NMR, specifically by the disappearance of the CH_2–Cl doublet and the formation of the CH_2–N doublet.

^{1}H NMR ($CDCl_3$ with 0.6 M pyridine, 600 MHz) δ 9.44 (d, J = 7.5 Hz, 2H, py), 8.43 (t, J = 7.5 Hz, 1H, py), 8.06 (t, J = 7.5 Hz, 2H, py), 5.59 (d, J = 7.6 Hz, 2H, CH_2–py), 5.45 (t, J = 7.6 Hz, 1H, C=CH), 1.98 (t, J = 7.6 Hz, 2H, C=C–CH_2), 1.82 (s, 3H, C=C–CH_3), 1.38–1.46 (m, 1H, CH), 1.37–1.27 (m, 2H, CH_2), 1.09–1.00 (m, 2H, CH_2), 0.83–0.73 (brm, 6H, CH_3).

HRMS calculated for $[C_{15}H_{24}N]^+$, requires m/z = 218.1909, found m/z = 218.1907 (ESI).

Formation of pyridinium **23A** from prenyl chloride was monitored by ^{1}H NMR, specifically by the disappearance of the CH_2–Cl doublet and the formation of the CH_2–N doublet.

^{1}H NMR ($CDCl_3$ with 0.6 M pyridine, 600 MHz) δ 9.58 (d, J = 3.9 Hz, 2H, py), 8.54 (t, J = 6.8 Hz, 1H, py), 8.18 (brt, J = 3.9 Hz, 2H, py), 5.66 (d, J = 6.5 Hz, 2H, CH_2–py), 5.56 (t, J = 6.8 Hz, 1H, C=CH), 1.93 (s, 3H, CH_3), 1.83 (s, 3H, CH_3).

HRMS calculated for $[C_{10}H_{14}N]^+$, requires m/z = 148.1126, found m/z = 148.1125 (ESI).

*Chloride **24** ((2E,6E)-8-Chloro-1-methoxy-2,6-dimethyl-2,6-octadiene).* The general procedure was followed using alcohol **24B** (109 mg, 0.592 mmol, 1 equiv), LiCl (30 mg, 0.71 mmol, 1.2 equiv), toluene (5 mL), DMF (2.4 mL, 0.25 M), 2,6-lutidine (270 µL, 2.36 mmol, 4.0 equiv), MsCl (92 µL, 1.2 mmol, 2.0 equiv), hexane (3 x 5 mL) and aqueous washes (5 mL each). Crude chloride **24** (102 mg, 0.502 mmol, 85% crude yield, pale yellow oil), which is not completely stable to silica gel, was assessed to be approximately 95% pure by NMR and was used directly for the subsequent experiments. ^{1}H NMR signals were assigned by ^{1}H–^{1}H COSY and by comparison to signals from the starting materials..

^{1}H NMR ($CDCl_3$, 600 MHz) δ 5.45 (t, J = 7.9 Hz, 1H, C=CH), 5.37 (t, J = 7.0 Hz, 1H, C=CH), 4.10 (d, J = 7.9 Hz, 2H, CH_2–Cl), 3.79 (s, 2H, CH_2–OMe), 3.27 (s, 3H, O–CH_3), 2.18 (q, J = 7.2 Hz, 2H, C=C–CH_2), 2.11 (t, J = 7.7 Hz, 2H, C=C–CH_2), 1.73 (s, 3H, CH_3), 1.64 (s, 3H, CH_3).

^{13}C NMR ($CDCl_3$, 150 MHz) δ 142.4, 132.8, 127.1, 120.8, 78.6, 57.5, 41.0, 39.2, 25.9, 16.1, 13.9.

IR (neat, cm^{-1}) 2927, 1659, 1455, 1253, 1113, 1098, 844, 665.

MS (decomposes under ESI conditions)

HRMS (decomposes under ESI conditions, analyzed as pyridinium adduct) calculated for $[C_{16}H_{24}ON]^+$, requires m/z = 246.1858, found m/z = 246.1861 (ESI).

TLC (5:1) hexane/EtOAc, permanganate, R_f = 0.59.

*Ether **24A** ((2E,6E)-8-Methoxy-3,7-dimethyl-2,6-octadienyl acetate)*. Into a flame-dried flask were added alcohol **12** (136 mg, 0.64 mmol, 1 equiv) and MeCN (1.0 mL, 0.6 M). The flask was fitted with a rubber septum and maintained under a nitrogen atmosphere. Into the flask were added silver oxide (296 mg, 1.28 mmol, 2.0 equiv) and then iodomethane (83 µL, 1.28 mmol, 2.0 equiv). The flask was fit with a reflux condenser, stirred in a 45 ºC oil bath (17 h), diluted with ethyl acetate (10 mL), filtered through a pad of Celite on silica gel, and dried with sodium sulfate. Volatiles were removed under reduced pressure, and the crude material (157 mg, full conversion by NMR, quantitative mass recovery) was used directly in the next step. For analysis, an aliquot was purified by column chromatography (silica gel, 5:1 hexane / EtOAc).

^{1}H NMR ($CDCl_3$, 600 MHz) δ 5.37 (t, J = 6.8 Hz, 1H, C=CH), 5.35 (t, J = 6.8 Hz, 1H, C=CH), 4.59 (d, J = 6.8 Hz, 2H, CH_2–OAc), 3.79 (s, 2H, CH_2–OMe), 3.27 (s, 3H, O–CH_3), 2.18 (q, J = 7.5 Hz, 2H, C=C–CH_2), 2.09 (t, J = 7.5 Hz, 2H, C=C–CH_2), 2.06 (s, 3H, Ac), 1.71 (s, 3H, CH_3), 1.64 (s, 3H, CH_3).

^{13}C NMR ($CDCl_3$, 150 MHz) δ 171.2, 142.0, 132.6, 127.4, 118.6, 78.6, 61.4, 57.4, 39.2, 25.9, 21.2, 16.5, 13.9.

IR (neat, cm^{-1}) 2927, 1738, 1230, 1092, 1028.

HRMS calculated for $[C_{13}H_{22}O_3Na]^+$, requires *m*/*z* = 249.1467, found *m*/*z* = 249.1461 (ESI).

TLC (4:1) hexane/EtOAc, permanganate, R_f = 0.63.

*Alcohol **24B** ((2E,6E)-8-Methoxy-3,7-dimethyl-2,6-octadien-1-ol)*. Into a flask were added crude acetate **24A** (0.64 mmol, 1 equiv), MeOH (2.4 mL, 0.3 M), and potassium carbonate (28 mg, 0.21 mmol, 0.3 equiv). The mixture was stirred (24 h), quenched with potassium phosphate monobasic (1 M aqueous, 5 mL, producing pH 5.0), and extracted with ethyl acetate (3 x 5 mL). The combined organic phase was washed with sodium chloride (50% saturated aqueous, 5 mL), and dried with sodium sulfate. Volatiles were removed under reduced pressure, and the crude material was purified by column chromatography (15 mL silica gel, 1:1 hexane / EtOAc) to yield pure alcohol **24B** (92 mg, 0.50 mmol, 78%, yield from alcohol **12**, colorless oil).

^{1}H NMR ($CDCl_3$, 600 MHz) δ 5.42–5.34 (m, 2H, 2 x C=CH), 4.14 (d, *J* = 7.0 Hz, 2H, CH_2–OH), 3.77 (s, 2H, CH_2–OMe), 3.27 (s, 3H, O–CH_3), 2.17 (q, *J* = 7.5 Hz, 2H, C=C–CH_2), 2.07 (t, *J* = 7.5 Hz, 2H, C=C–CH_2), 1.67 (s, 3H, CH_3), 1.63 (s, 3H, CH_3), 1.52–1.48 (brs, 1H, OH).

^{13}C NMR ($CDCl_3$, 150 MHz) δ 139.1, 132.4, 127.8, 123.9, 78.8, 59.4, 57.5, 39.2, 26.0, 16.3, 13.9.

IR (neat, cm^{-1}) 3389, 2927, 1449, 1092, 999.

HRMS calculated for $[C_{11}H_{20}O_2Na]^+$, requires *m*/*z* = 207.1361, found *m*/*z* = 207.1357 (ESI).

TLC (3:1) hexane/EtOAc, permanganate, R_f = 0.23.

Formation of pyridinium **24C** from chloride **24** was monitored by ^{1}H NMR, specifically by the disappearance of the CH_2–Cl doublet and the formation of the CH_2–N doublet.

^{1}H NMR ($CDCl_3$ with 0.6 M pyridine, 600 MHz) δ 9.37 (brs, 2H, py), 8.41 (t, *J* = 7.3 Hz, 1H, py), 8.01 (t, *J* = 7.3 Hz, 2H, py), 5.53 (d, *J* = 7.3 Hz, 2H, CH_2–py), 5.41 (t, *J* = 7.3 Hz, 1H, C=CH), 5.19 (brs, 1H, C=CH), 3.60 (s, 2H, CH_2–OMe), 3.12 (s, 3H, O–CH_3), 2.05 (brs, 4H, 2 x C=C–CH_2), 1.78 (s, 3H, CH_3), 1.46 (s, 3H, CH_3).

HRMS calculated for $[C_{16}H_{24}ON]^+$, requires *m*/*z* = 246.1858, found *m*/*z* = 246.1861 (ESI).

Acknowledgements

Financial support was provided by Clark University. We would like to thank Prof. Ksenia Bravaya and Prof. Ming Lei for helpful discussions on the computational aspects of this work.

Supporting Information

NMR spectra and results from kinetics experiments, computational methods, calculated orbital structures and energies, NMR spectra from synthesis, atomic coordinates of computed structures.

[1] Dewick, P. *Nat. Prod. Rep.* **2002**, *19*, 181–222.

[2] Corey, E. J.; Ohno, M.; Vatakencherry, P. A.; Mitra, R. B. *J. Am. Chem. Soc.* **1961**, *83*, 1251–1253.

[3] Chen, K.; Baran, P. S. *Nature* **2009**, *459*, 824–828.
[4] McKerrall, S. J.; Jorgensen, L.; Kuttruff, C. A.; Ungeheuer, F.; Baran, P. S. *J. Am. Chem. Soc.* **2014**, *136*, 5799–5810.
[5] Guilford, W. J.; Coates, R. M. *J. Am. Chem. Soc.* **1982**, *104*, 3506–3508.
[6] Rodríguez, A. D.; González, E.; Ramírez, C. *Tetrahedron* **1988**, *54*, 11683–11729.
[7] Adio, A. M. *Tetrahedron* **2009**, *65*, 1533–1552.
[8] Takamura, H.; Kikuchi, T.; Endo, N.; Fukuda, Y.; Kadota, I. *Org. Lett.* **2016**, *18*, 2110–2113.
[9] Trotta, A. H. *Org. Lett.* **2015**, *17*, 3358–3361.
[10] Yang, Z.–J.; Ge, W.–Z.; Li, Q.–Y.; Lu, Y.; Gong, J.–M.; Kuang, B.–J.; Xi, X.; Wu, H.; Zhang, Q.; Chen, Y. *J. Med. Chem.* **2015**, *58*, 7007–7020.
[11] Reardon, M. B.; Yasgur, B. C.; Jakobsche, C. E. *Tetrahedron Lett.* **2016**, *57*, 2782–2785.
[12] Reardon, M. B.; Carlson, G. W.; Jakobsche, C. E. *Synthesis* **2014**, *46*, 387–393
[13] Hammett, L. P.; *Chem. Rev.* **1935**, *17*, 125–136.
[14] Song, I. H.; le Noble, W. J. *J. Org. Chem.* **1994**, *59*, 58–66.
[15] Mehta, G.; Khan, F. A. *J. Am. Chem. Soc.* **1990**, *112*, 6140–6142.
[16] (a) Yu, X.–J.; Zhang, H.; Xiong, F.–J.; Chen, X.–X.; Chen, F.–E. *Helv. Chem. Acta.* **2008**, *91*, 1967–1974. (b) Umbreit, M. A.; Sharpless, K. B. *J. Am. Chem. Soc.* **1977**, *99*, 5526–5528.
[17] Manchand, P. S.; Yiannikouros, G. P.; Belica, P. S.; Madan, P. *J. Org. Chem.* **1995**, *60*, 6574–6581.
[18] Choudhary, A.; Gandla, D.; Krow, G. R.; Raines, R. T. *J. Am. Chem. Soc.* **2009**, *131*, 7244–7246.
[19] Pophristic, V.; Goodman, L. *Nature* **2001**, *411*, 565–568.
[20] Gaussian 09, Revision E.01, Frisch, M. J.; Trucks, G. W.; Schlegel, H. B.; Scuseria, G. E.; Robb, M. A.; Cheeseman, J. R.; Scalmani, G.; Barone, V.; Mennucci, B.; Petersson, G. A.; Nakatsuji, H.; Caricato, M.; Li, X.; Hratchian, H. P.; Izmaylov, A. F.; Bloino, J.; Zheng, G.; Sonnenberg, J. L.; Hada, M.; Ehara, M.; Toyota, K.; Fukuda, R.; Hasegawa, J.; Ishida, M.; Nakajima, T.; Honda, Y.; Kitao, O.; Nakai, H.; Vreven, T.; Montgomery, J. A., Jr.; Peralta, J. E.; Ogliaro, F.; Bearpark, M.; Heyd, J. J.; Brothers, E.; Kudin, K. N.; Staroverov, V. N.; Kobayashi, R.; Normand, J.; Raghavachari, K.; Rendell, A.; Burant, J. C.; Iyengar, S. S.; Tomasi, J.; Cossi, M.; Rega, N.; Millam, J. M.; Klene, M.; Knox, J. E.; Cross, J. B.; Bakken, V.; Adamo, C.; Jaramillo, J.; Gomperts, R.; Stratmann, R. E.; Yazyev, O.; Austin, A. J.; Cammi, R.; Pomelli, C.; Ochterski, J. W.; Martin, R. L.; Morokuma, K.; Zakrzewski, V. G.; Voth, G. A.; Salvador, P.; Dannenberg, J. J.; Dapprich, S.; Daniels, A. D.; Farkas, Ö.; Foresman, J. B.; Ortiz, J. V.; Cioslowski, J.; Fox, D. J. Gaussian, Inc., Wallingford CT, 2009.
[21] (a) Becke; A. D. *J. Chem. Phys.* **1993**, *98*, 5648–5652. (b) Lee, C.; Yang, W.; Parr, R. G. *Phys. Rev. B* **1988**, *37*, 785–789. (c) Vosko, S. H.; Wilk, L.; Nusair, M. *Can. J. Phys.* **1980**, *58*, 1200–1211. (d) Stephens, P. J.; Devlin, F. J.; Chabalowski, C. F.; Frisch, M. J. *J. Phys. Chem*. **1994**, *98*, 11623–11627.
[22] (a) Binning R. C. Jr.; Curtiss, L. A. *J. Comp. Chem.* **1990**, *11,* 1206–1216. (b) McGrath, M. P.; Radom, L. *J. Chem. Phys*. **1991**, *94* 511–516. (c) Curtiss, L. A.; Jones, C.; Trucks, G. W.; Raghavachari, K. *J. Chem. Phys.* **1990**, *93*, 2537–2545.
[23] (a) Miertuš, S.; Scrocco, E.; Tomasi, J. *Chem. Phys.*, **1981**, *55*, 117–129. (b) Tomasi, J.; Mennucci, B.; Cammi, R. *Chem. Rev.*, **2005**, *105*, 2999–3093.
[24] Zhao, Y.; Truhlar, D. G. *Theor. Chem. Account* **2006**, *120*, 215–241.

[25] Clark, T.; Chandrasekhar, J.; Spitznagel, G. W.; von Ragué Schleyer, P. *J. Comp. Chem.*, **1983**, *4*, 294–301.
[26] Clemente F. R.; Houk, K. N. *Angew. Chem.; Int. Ed.*, **2004**, *43*, 5766 –5768.
[27] *Molecular Operating Environment (MOE)*, 2013.08; Chemical Computing Group Inc., 1010 Sherbooke St. West, Suite #910, Montreal, QC, Canada, H3A 2R7, **2016**.
[28] Labute, P. *J. Chem. Inf. Model.* **2010**, *50*, 792–800.
[29] (a) Gerber, P. R.; Muller, K. *J. Comput. Aided Mol. Des.* **1995**, *9*, 251–268. (b) Case, D. A.; Cheatham, T. E. III; Darden, T.; Gohlke, H.; Luo, R.; Merz, K. M. Jr.; Onufriev, A.; Simmerling, C.; Wang, B.; Woods, R. J. *J. Comput. Chem.* **2005**, *26*, 1668–1688.
[30] Pettersen, E. F.; Goddard, T. D.; Huang, C. C.; Couch, G. S.; Greenblatt, D. M.; Meng, E. C.; Ferrin, T. E. *J. Comput. Chem.* **2004** *25*, 1605–1612.
[31] Jakobsche, C. E.; Choudhary, A.; Miller, S. J.; Raines, R. T. *J. Am. Chem. Soc.* **2010**, *132*, 6651–6653.
[32] Hoyle, J.; Grossert, S. J.; Hooper, D. L.; Sotheeswaran, S. *Can. J. Chem.* **1986**, *64*, 1581–1584.
[33] Motherwell, W. B.; Begis, G.; Cladingboel, D. E.; Jerome, L.; Sheppard, T. D. *Tetrahedron* **2007**, *63*, 6462–6476.
[34] Takashi, K. World Patent Application WO/2009/057668, July 5, 2009.
[35] Fang, L.; Xue, H.; Yang, J. *Org. Lett.* **2008**, *10*, 4645–4648.